AD-A125 213 NUMERICAL DYNAMIC ANALYSIS OF STRUCTURES BY THE FINITE DYNAMIC ELEMENT METHOD(U) JET PROPULSION LAB PASADENA CA K K GUPTA 15 AUG 82 AFOSR-TR-82-1095 AFOSR-80-0169 1/1

UNCLASSIFIED F/G 12/1 NL

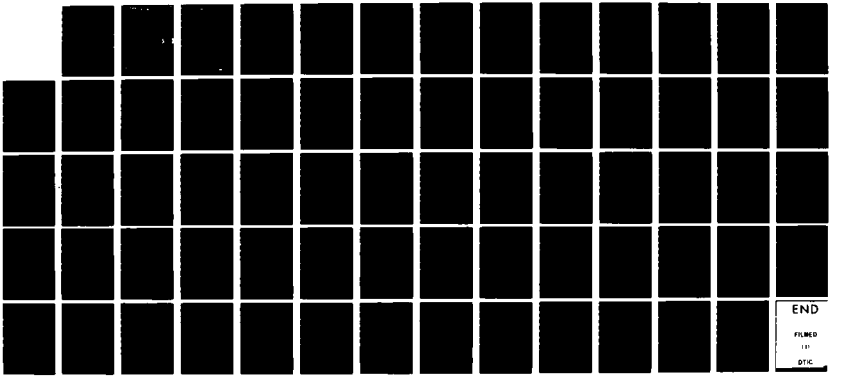

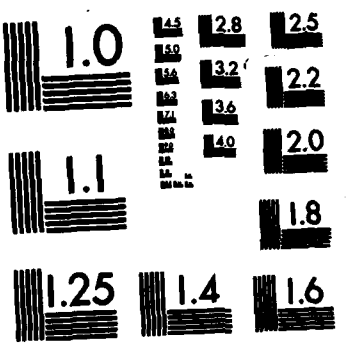

UNCLASSIFIED

SECURITY CLASSIFICATION OF THIS PAGE (When Data Entered)

(3)

REPORT DOCUMENTATION PAGE	READ INSTRUCTIONS BEFORE COMPLETING FORM
1. REPORT NUMBER: AFOSR-TR- 82-1095	2. GOVT ACCESSION NO.: A125213
3. RECIPIENT'S CATALOG NUMBER	
4. TITLE (and Subtitle): NUMERICAL DYNAMIC ANALYSIS OF STRUCTURES BY THE FINITE DYNAMIC ELEMENT METHOD	5. TYPE OF REPORT & PERIOD COVERED: Final: 01 Feb 80 - 15 Aug 82
	6. PERFORMING ORG. REPORT NUMBER
7. AUTHOR(s): Kajal K. Gupta	8. CONTRACT OR GRANT NUMBER(s): AFOSR-80-0169
9. PERFORMING ORGANIZATION NAME AND ADDRESS: Jet Propulsion Laboratory, California Institute of Technology, Pasadena, California	10. PROGRAM ELEMENT, PROJECT, TASK AREA & WORK UNIT NUMBERS: 61102F 2304/A3
11. CONTROLLING OFFICE NAME AND ADDRESS: Mathematical and Information Sciences Directorate, Air Force Office of Scientific Research, Bolling AFB, DC 20332	12. REPORT DATE: 15 AUGUST 1982
	13. NUMBER OF PAGES: 65
14. MONITORING AGENCY NAME & ADDRESS (if different from Controlling Office)	15. SECURITY CLASS. (of this report): Unclassified
	15a. DECLASSIFICATION/DOWNGRADING SCHEDULE

16. DISTRIBUTION STATEMENT (of this Report)

Approved for public release;
distribution unlimited.

DTIC ELECTE S MAR 3 1983 D B

17. DISTRIBUTION STATEMENT (of the abstract entered in Block 20, if different from Report)

18. SUPPLEMENTARY NOTES

19. KEY WORDS (Continue on reverse side if necessary and identify by block number)

20. ABSTRACT (Continue on reverse side if necessary and identify by block number)

This report describes progress made in research during the final year of a five-year study of numerical dynamical analysis of structures funded by an AFOSR Grant. The original proposal was JPL Proposal 51-641 dated 6-29-76, and the final year renewal was proposed on 12-18-80.

The proposed work effort in the final year's work included the following Tasks: (I) development of a higher order rectangular plane stress/strain finite element, (II) development of a solid hexahedron finite dynamic element, (III) further refinement of the Associated Generalized

-over-

DD FORM 1 JAN 73 1473

cont

UNCLASSIFIED

SECURITY CLASSIFICATION OF THIS PAGE (When Data Entered)

UNCLASSIFIED

Item 20 continued: Eigenproblem Solution Routine.

UNCLASSIFIED

AFOSR-TR- 82-1095

(3)

NUMERICAL DYNAMIC ANALYSIS OF STRUCTURES BY THE FINITE DYNAMIC ELEMENT METHOD

AFOSR
FINAL REPORT ON AFOSR GRANT NO. 80-0169
JPL Proposal No. 51-641

August 15, 1982

Kajal K. Gupta
Principal Investigator

to the
AIR FORCE OFFICE SCIENTIFIC RESEARCH
DIRECTORATE OF MATHEMATICAL AND INFORMATION SCIENCES (AFOSR/NM)

Jet Propulsion Laboratory
California Institute of Technology
Pasadena, California

TABLE OF CONTENTS

SUMMARY

This report describes progress made in research during the final year of a five-year study of numerical dynamical analysis of structures funded by an AFOSR Grant. The original proposal was JPL Proposal 51-641 dated 6-29-76, and the final year renewal was proposed on 12-18-80.

The proposed work effort in the final year's work included the following Tasks:

Task I - Development of a higher order rectangular plane stress/strain finite element.

Task II - Development of a solid hexahedron finite dynamic element.

Task III - Further refinement of the Associated Generalized Eigenproblem Solution Routine.

The nature of this work is to generate analytical results for publication in the open literature. It is common procedure, therefore, to report the results of contractural work by submitting preprints or reprints of articles to be published as the result of research supported under these tasks. We have therefore collected together the appropriate preprints and reprints and packaged them together as the report for the final year's effort.

In addition to this work in strict adherance with the Task descriptions, a piece of research was carried out on the application of the finite dynamic element method to coupled fluid-structure problems. This was done at the invitation of the Fourth International Symposium on Finite Element Methods in Flow Problems, and represents a logical extension of developments within the AFOSR Grant to new application areas of interest to the Air Force.

The report is therefore divided into four parts:

Task I - Higher order element

Task II - Solid hexahedron element

Task III - Refinement of the solution routine

Task IV - Application to fluid-structure problems

REPORT ON TASK I

"Development of a Higher-Order Plane Finite Dynamic Element"

(to be published)

NUMERICAL FORMULATION FOR A HIGHER-ORDER PLANE FINITE DYNAMIC ELEMENT

K. K. Gupta

SUMMARY

The paper is essentially concerned with the development of a 8-node plane, rectangular finite dynamic element and presents detailed descriptions of the associated numerical formulation involving the higher order dynamic correction terms, pertainings to the related stiffness and inertia matrices.

Numerical test results of free vibration analysis are presented in detail, for the newly developed 8-node element, as well as the corresponding 4-node element to afford a clear comparison of the relative efficiences of the corresponding finite element and the dynamic element procedures. Such results indicate a superior pattern of solution convergence of the presently developed dynamic element.

INTRODUCTION

A discrete element idealization of a continuum, undergoing free vibration, may be achieved by uniquely relating the displacement field within an element in terms of its nodal values. Such a relationship is expressed as

$$\underline{u} = \underline{a}(\omega)\,\underline{U} \tag{1}$$

in which the shape function matrix $\underline{a}$ is a function of the natural frequencies ω, of the structure under consideration. The associated stiffness and inertia matrices may then be derived by standard procedures, based on variational principles, noting that the resulting matrices are obtained as functions of the initially unknown natural frequencies. Subsequent extraction of roots and vectors from these matrices is extremely difficult and uneconomical in nature and to avoid such a unwieldy formulation equation (1) is expanded in ascending powers of ω, as below:

$$\underline{a}(\omega) = \underline{a}_0 + \omega\underline{a}_1 + \omega^2\underline{a}_2 + \ldots \tag{2}$$

resulting in the following expressions for the element stiffness and inertia matrices

$$\underline{K} = \underline{K}_0 + \omega^2\underline{K}_2 + \omega^4\underline{K}_4 + \ldots \tag{3}$$

$$\underline{M} = \underline{M}_0 + \omega^2\underline{M}_2 + \omega^4\underline{M}_4 + \ldots \tag{4}$$

These matrices when appropriately combined yields the global matrices for the entire continuum. The associated free vibration formulation is given by

$$[\underline{K}_0 - \omega^2(\underline{M}_0 - \underline{K}_2) - \omega^4(\underline{M}_2 - \underline{K}_4) - \ldots]\,\underline{q} = \underline{0} \tag{5}$$

in which the higher order dynamic correction matrices $\underline{K}_2$, $\underline{K}_4$, $\underline{M}_2$ and such other terms are retained in the formulation in the dynamic element method (DEM), whereas only the initial terms $\underline{K}_0$ and $\underline{M}_0$ are included in the analysis employing the usual finite element method (FEM). Furthermore, in the dynamic element procedure, the series form of equation (5) is suitably truncated to yield a quadratic matrix eigenvalue problem

$$(\underline{A}-\lambda\underline{B}-\lambda^2\underline{C})\ \underline{q} = \underline{0} \tag{6}$$

with $\underline{A} = \underline{K}_0$, $\underline{B} = \underline{M}_0-\underline{K}_2$, $\underline{C} = \underline{M}_2-\underline{K}_4$ and $\lambda = \omega^2$, whereas in the finite element method the equivalent formulation has the form

$$(\underline{A}-\lambda\underline{B})\ \underline{q} = \underline{0} \tag{7}$$

where

$$\underline{B} = \underline{M}_0 \ .$$

A dynamic element formulation was earlier achieved for line elements[1], involving derivation of the higher order dynamic correction terms. The procedure was further developed for continuum discretization and details of the relevant dynamic elements pertaining to membrane[2] and plane stress[3,4] problems have been published earlier. Such results indicate that dynamic elements exhibit much superior solution convergence characteristics when compared with the usual finite element method, resulting in substantial economy in the free vibration analysis of practical problems. Furthermore, the usual solution techniques[5] for the quadratic matrix equation involved the eigenproblem solution of an equivalent system characterized by a single full matrix of order twice that of the original system, requiring prohibitive computational effort for most practical problems. However, new solution techniques[6,7] for the quadratic matrix formulation of equation (6) pertaining to the dynamic element method enable eigenproblem solution with approximately the same computational effort as that required for the solution of equation (7) associated with a finite element formulation.

The purpose of this paper is to present detailed formulation of a 8-node, plane rectangular dynamic element. Numerical results are presented for a representative problem, solved by both the DEM and FEM formulation. Furthermore, similar results are presented for the corresponding 4-node element to afford a clear comparison of convergence characteristics of the various element types.

DYNAMIC ELEMENT FORMULATION FOR A PLANE 8-NODE RECTANGULAR ELEMENT

Figure 1 depicts a typical rectangular, 8-node plane element. The differential equations of free vibration of such a continuum are of the following form

$$\frac{\partial^2 u_x}{\partial x^2} + \frac{\partial^2 u_x}{\partial y^2} + \frac{1}{(1-2\mu)} \frac{\partial}{\partial x}\left(\frac{\partial u_x}{\partial x} + \frac{\partial u_y}{\partial y}\right) = 2(1+\mu)\frac{\rho}{E}\frac{\partial^2 u_x}{\partial t^2} \tag{8}$$

$$\frac{\partial^2 u_y}{\partial x^2} \quad \frac{\partial^2 u_y}{\partial y^2} + \frac{1}{(1-2\mu)} \frac{\partial}{\partial y}\left(\frac{\partial u_x}{\partial x} + \frac{\partial u_y}{\partial y}\right) = 2(1+\mu)\frac{\rho}{E}\frac{\partial^2 u_y}{\partial t^2} \tag{9}$$

where ρ, μ and E are the element mass per unit area, Poisson's ratio and the Young's modulus, respectively. Appropriate solution of equations (8) and (9) for the in-plane deformations u_x, u_y may be expressed in infinite series form as below

$$u_y = \underline{a}(\omega)\underline{U} = (\underline{a}_{0x} + \omega\underline{a}_{1x} + \omega^2\underline{a}_{2x} + \ldots)\,\underline{U} \tag{10}$$

$$u_y = \underline{a}(\omega)\underline{U} = (\underline{a}_{0y} + \omega\underline{a}_{1y} + \omega^2\underline{a}_{2y} + \ldots)\,\underline{U} \tag{11}$$

which if substituted in equations (8) and (9) yields the final expressions for the differential equations. As for example, such equations in the y-direction are as follows

$$\frac{\partial^2 \underline{a}_{0y}}{\partial x^2} + \frac{\partial^2 \underline{a}_{0y}}{\partial y^2} + \alpha_2 \frac{\partial^2 \underline{a}_{0y}}{\partial y^2} + \frac{\partial^2 \underline{a}_{0y}}{\partial x \partial y} = 0 \tag{12}$$

$$\frac{\partial^2 \underline{a}_{1y}}{\partial x^2} + \frac{\partial^2 \underline{a}_{1y}}{\partial y^2} + \alpha_2 \frac{\partial^2 \underline{a}_{1y}}{\partial y^2} + \frac{\partial^2 \underline{a}_{1n}}{\partial x \partial y} = 0 \tag{13}$$

$$\alpha_1 \frac{\partial^2 \underline{a}_{2y}}{\partial y 2} + \frac{\partial^2 \underline{a}_{2y}}{\partial x 2} + \alpha_2 \frac{\partial^2 \underline{a}_{2x}}{\partial x \partial y} = -\beta \underline{a}_{0y} \tag{14}$$

in which

$$\alpha_1 = \frac{2(1-\mu)}{(1-2\mu)}, \quad \alpha_2 = \frac{1}{(1-2\mu)} \quad \text{and} \quad \beta = \frac{2\rho}{E}(1+\mu),$$

similar expressions being also obtained in the x direction.

When solving such differential equations, it is postulated that while $\underline{a}_0$ is allowed to satisfy the appropriate boundary conditions $\underline{a}_1$ and $\underline{a}_2$ must all vanish at the boundaries. Thus the solutions for $\underline{a}_{0x}$, $\underline{a}_{0y}$ satisfying equation (1) and its counterpart are assumed as below

$$\underline{a}_{0x} = c_1 + c_2 x + c_3 y + c_4 x^2 + c_5 xy + c_6 y^2 + c_7 x^2 y + c_8 xy^2 \tag{15}$$

$$\underline{a}_{0y} = c_9 + c_{10} x + c_{11} y + c_{12} x^2 + c_{13} xy + c_{14} y^2 + c_{15} x^2 y + c_{16} xy^2 \tag{16}$$

in which the coefficients $c_1 - c_{16}$ are evaluated by satisfaction of the boundary conditions

$u_x = U_1$, $u_y = U_2$ at $x = 0$, $y = 0$ $\quad u_x = U_3$, $u_y = U_4$ at $x = 2a$, $y = 0$

$u_x = U_5$ $u_y = U_6$ at $x = 2a$, $y = 2b$ $u_x = U_7$, $u_y = U_8$ at $x = 0$, $y = 2b$

$u_x = U_9$ $u_y = U_{10}$ at $x = a$, $y = 0$ $\quad u_x = U_{11}$, $u_y = U_{12}$ at $x = 2a$, $y = b$

$u_x = U_{13}$ $u_y = U_{14}$ at $x = a$, $y = 2b$ $u_x = U_{15}$, $u_y = U_{16}$ at $x = 0$, $y = b$

Expressions, similar to equations (15) and (16) are chosen as solutions for $\underline{a}$, yielding $\underline{a}_{1x} = \underline{0}$, $\underline{a}_{1y} = \underline{0}$; appropriate solutions for equation (14) and its counterpart, on the other hand, are assumed as follows

$$\underline{a}_{2x} = \hat{c}_1 + \hat{c}_{2x} + \hat{c}_{3y} + \hat{c}_4 x^2 + \hat{c}_5 xy + \hat{c}_6 y^2 + \hat{c}_7 x^2 y + \hat{c}_8 xy^2$$

$$-\rho \left[\frac{c_1}{4} \frac{x^2}{\alpha_1} + \frac{c_1}{4} y^2 + \frac{c_2 x^3}{12\alpha_1} + \frac{c_2}{4} \frac{xy^2}{4} + \frac{c_3}{4} \frac{x^2 y}{\alpha_1} + \frac{c_3 y^3}{12} + \frac{c_4}{24} \frac{x^4}{\alpha_1} + \frac{c_4}{4} \frac{x^2 y^2}{} \right.$$

$$\left. + \frac{c_5}{12} \frac{x^3 y}{\alpha_1} + \frac{c_5 xy^3}{12} + \frac{c_6 x^2 y^2}{4 \alpha_1} + \frac{c_6 y^4}{24} + \frac{c_7}{24} \frac{x^4 y}{\alpha_1} + \frac{c_7 x^2 y^3}{12} + \frac{c_8}{12} \frac{x^3 y^2}{\alpha_1} + \frac{c_8 xy^4}{24} \right] \tag{17}$$

$$\underline{a}_{2y} = \hat{c}_9 + \hat{c}_{10} x + \hat{c}_{11} y + \hat{c}_{12} x^2 + \hat{c}_{13} xy + \hat{c}_{14} y^2 + \hat{c}_{15} x^2 y + \hat{c}_{16} xy^2$$

$$-\beta \left[\frac{c_9}{4} \frac{y^2}{\alpha_1} + \frac{c_9}{4} x^2 + \frac{c_{10}}{4} \frac{xy^2}{\alpha_1} + \frac{c_{10}}{12} x^3 + \frac{c_{11}}{12} \frac{y^3}{\alpha_1} + \frac{c_{11}}{4} x^2 y + \frac{c_{12}}{4} \frac{x^2 y^2}{\alpha_1} + \frac{c_{12}}{24} x^4 \right.$$

$$+ \frac{c_{13}}{12} \frac{xy^3}{\alpha_1} + \frac{c_{13}}{12} x^3 y + \frac{c_{14}}{24} \frac{y^4}{\alpha_1} + \frac{c_{14}}{4} x^2 y^2 + \frac{c_{15}}{12} \frac{x^2 y^3}{\alpha_1} + \frac{c_{15}}{24} x^4 y + \frac{c_{16}}{24} \frac{xy^4}{\alpha 1}$$

$$\left. + \frac{c_{16}}{12} x^3 \right] \tag{18}$$

when the coefficients $\hat{c}_1 - \hat{c}_{16}$ of the complementary functions are determined by satisfying the appropriate boundary conditions, noting that the coefficients $c_1 - c_{16}$ are computed earlier from equations (15) and (16). The final forms of the shape functions are obtained after performing some routine algebraic manipulations. Appropriate derivations of the higher order shape function matrix $\underline{a}_2$ is crucial in the development of the current finite dynamic element.

The shape function vectors are thus defined as

$$\underline{a}_x = \underline{a}_{0x} + \omega^2 \underline{a}_{2x} \ , \quad \underline{a}_y = \underline{a}_{0y} + \omega^2 \underline{a}_{2y} \tag{19}$$

in which the scalars of each vector are coupled to the appropriate nodal degrees of freedom of the element. Associated strain-displacement relationship is given as

$$\underline{e} = \underline{b}\,\underline{U} = (\underline{b}_0+\omega^2\underline{b}_2)\,U \tag{20}$$

in which

$$\underline{e}_{xx} = \frac{\partial \underline{u}_x}{\partial x} = \frac{\partial}{\partial x}(\underline{a}_{0x}+\omega^2\underline{a}_{2x})\,\underline{U} = (\underline{b}_{0xx}+\omega^2\underline{b}_{2xx})\,\underline{U}$$

$$\underline{e}_{yy} = \frac{\partial \underline{u}_y}{\partial y} = \frac{\partial}{\partial y}(\underline{a}_{0y}+\omega^2\underline{a}_{2y})\,U = (\underline{b}_{0yy}+\omega^2\underline{b}_{2yy})\,\underline{U}$$

$$e_{xy} = \frac{\partial u_x}{\partial y} + \frac{\partial u_y}{\partial x} = \left(\frac{\partial \underline{a}_{0x}}{\partial y} + \frac{\partial \underline{a}_{0y}}{\partial x}\right)\underline{U} + \omega^2\left(\frac{\partial \underline{a}_{2x}}{\partial y} + \frac{\partial \underline{a}_{2y}}{\partial x}\right)$$
$$= (b_{0xy} + \omega^2 b_{2xy})\,\underline{U} \tag{21}$$

The individual strain-displacement matrices are suitably combined to yield the $\underline{b}_0$ and $\underline{b}_2$ matrices.

The element stiffness and inertia matrices may next be developed by standard procedure once the various $\underline{a}$ and $\underline{b}$ matrices have been determined, as above. Thus the stiffness matrix is obtained as

$$\underline{K} = \underline{K}_0 + \omega^4\,\underline{K}_4 \tag{22}$$

where

$$\underline{K}_0 = \int_\nu \underline{b}_0{}^T \underline{x}\,\underline{b}_0\,dv \tag{23}$$

$$\underline{K}_t = \int_\nu \underline{b}_2{}^T \underline{x}\,\underline{b}_2\,dv \tag{24}$$

and in which $\underline{x}$ is the stress-strain matrix for two dimensional elasticity, ν being volume of the element. In a similar manner the inertia matrices are given as

$$\underline{m}_x = \underline{m}_{0x} + \omega^2\underline{m}_{2x} \tag{25}$$

$$\underline{m}_y = \underline{m}_{0y} + \omega^2\underline{m}_{2y} \tag{26}$$

in which

$$\underline{m}_{0x} = \rho_\nu \int_\nu \underline{a}_{0x}^T \underline{a}_{0x}\, dv \tag{27}$$

$$\underline{m}_{2x} = \rho_\nu \int_\nu \underline{a}_{0x}^T \underline{a}_{2x}\, dv + \rho_\nu \int_\nu \underline{a}_{2x}^T \underline{a}_{0x}\, dv \tag{28}$$

$$\underline{m}_{0y} = \rho_\nu \int_\nu \underline{a}_{0y}^T \underline{a}_{0y}\, dv \tag{29}$$

$$\underline{m}_{2y} = \rho_\nu \int_\nu \underline{a}_{0y}^T \underline{a}_{2y}\, dv + \rho_\nu \int_\nu \underline{a}_{2y}^T \underline{a}_{0y}\, dv \tag{30}$$

where ρ_ν is the mass per unit volume of the plate element.

The symbolic manipulation program MACSYMA[8], has been utilized in processing equations (15)-(30) for the derivation of the $\underline{a}$, $\underline{b}$, $\underline{m}$ and $\underline{K}$ matrices involving rather large amounts of algebraic manipulations. The resulting expression for the matrix elements are next transformed in FORTRAN programmed form, by employing a suitable MACSYMA instruction. Due to the lengthy nature of the expressions for $\underline{a}$, $\underline{b}$, $\underline{m}$, and $\underline{K}$ matrices, they are not reproduced here for ready reference; however, the programmed form of these individual expressions may be supplied for appropriate utilization. The element matrices are then combined by standard process to yield the global stiffness, inertia and dynamic correction matrices for subsequent analysis of numerical examples, by solving the quadratic eigenvalue problem depicted by equation 6.

NUMERICAL RESULTS

A square plate, (Figure 2) with one edge fixed and three edges free, vibrating in its own plane, is chosen as a numerical example as before[3,4], having the following basic structural data: side length (l) = 10.0, thickness (t) = 1.0; Poisson's ratio (μ) = 0.3. Solution results were obtained for the model employing an increasing number of elements and such analyses were performed for both the dynamic and the finite element idealizations. Table I presents these results in parametric form, along with similar results obtained by utilizing 4-node rectangular elements[3]. Such a table, on the other hand, provides a clear comparison of the pattern of root convergence of the higher-order 8-node and the simple 4-node dynamic and finite elements, in a concised form.

Figure 3 depicts the pattern of convergence of two typical roots pertaining to the four sets of results, for varying mesh sizes. Such results are also depicted in Figure 4, as a function of total computational effort involved in the respective eigenproblem solution. The solution results pertaining to a 20 x 20 mesh discretization is accepted as the exact solution, in the absence of an available analytical solution.

CONCLUDING REMARKS

Numerical results presented in Table I are further depicted in Figures 3 and 4 to provide a better insight into the patterns of behavior of the newly developed 8-node dynamic element as well as its finite element counterpart. Such results are also presented for the simple 4-node element to afford a clear comparison of the relative solution efficiencies for both the elements employing either the dynamic element or the finite element technique. It is quite apparent from these results that significant improvement in root convergence is achieved when dynamic elements are used in place of the usual finite elements. Furthermore, Figure 4 indicates that a 4-node dynamic element displays convergence characteristics similar to an 8-node finite element. Thus, for a required two percent solution accuracy for ω_5 the eigenproblem solution efforts for the 8-node DEM/FEM and 4-node DEM/FEM procedures bear the ratios 1,6,4 and 15 respectively. Also, with increasing mesh size, errors in frequencies computed by the DEM analysis decrease much more rapidly than the FEM computations. Furthermore, for a given solution accuracy, the DEM analysis requires considerably less data preparation effort due to a significant reduction in mesh size.

As pointed out in the Introduction section, the development of the dynamic elements proved to be highly beneficial only after new eigenproblem solution techniques were formulated that enable solution of the quadratic matrix equation $(\underline{A} - \omega^2 \underline{B} - \omega^2 \underline{C})\ \underline{q} = \underline{0}$. A discussion on the choice of the higher order shape function, which is crucial to the current formulation, is given elsewhere[4].

REFERENCES

1. J.S. Przemieniecki, Theory of Matrix Structural Analysis, McGraw-Hill, New York, 1968.

2. K.K. Gupta, 'On a finite dynamic element method for free vibration analysis of structures', Comput. Meth. Appl. Mech. Eng. 9 105-20 (1976).

3. K.K. Gupta, 'Development of a finite dynamic element for free vibration of two-dimensional structures', Int. J. num. Them. Eng. 12 1311-27 (1978).

4. K.K. Gupta, 'Finite dynamic element formulation for a plane triangular element', Int. J. num. Meth. Eng. 14 1431-1448 (1979).

5. J.H. Wilkinson, The Algebraic Eigenvalue Problem, Clarendon Press, Oxford, 1965.

6. K.K. Gupta, 'Numerical solution of quadratic matrix equations for free vibration analysis of structures', 3rd Post Conference on Computational Aspects of the Finite Element Method, Dept. of Aeronautics, Imperial College, London (1975).

7. K.K. Gupta, "Development of a unified numerical procedure for free vibration analysis of structures, Int. J. num. Meth. Eng., 17, 187-198 (1981).

8. R. Bogen, MACSYMA Reference Manual, The Mathlab Group, Massachusetts Institute of Technology, Cambridge, Massachusetts, 1975.

Table I

Comparison of natural frequency values of a square cantilever plate (FEM and DEM results for 8-node elements shown in upper and lower rows, corresponding values for 4-node elements shown in parenthesis)

	Eigenvalue Parameter $\hat{\omega} = \omega / (E/\rho)$					
Mesh Size	$\hat{\omega}_1$	$\hat{\omega}_2$	$\hat{\omega}_3$	$\hat{\omega}_4$	$\hat{\omega}_5$	$\hat{\omega}_6$
1x1	.07046	.1602	.1926	.3169	.3867	.3968
	(.07792)	(.1743)	(.2908)			
	.07027	.1522	.1736	.2715	.3182	.3708
	(.07444)	(.1491)	(.2444)			
2x2	.06708	.1585	.1817	.2906	.3167	.3289
	(.07186)	(.1637)	(.2090)	(.3372)	(.3905)	(.3964)
	.06706	.1579	.1797	.2801	.3058	.3077
	(.07096)	(.1547)	(.1946)	(.2960)	(.3340	(.3441)
3x3	.0638	.1583	.1785	.2835	.3083	.3235
	(.06913)	(.1608)	(.1934)	(.3152)	(.3500)	(.3609)
	.06636	.1582	.1781	.2803	.3049	.3181
	(.06876)	(.1565)	(.1867)	(.2923)	(.3190)	(.3288)
20x20 (exact results)	(.06585)	(.1579)	(.1769)	(.2796)	(.3033)	(.3214)

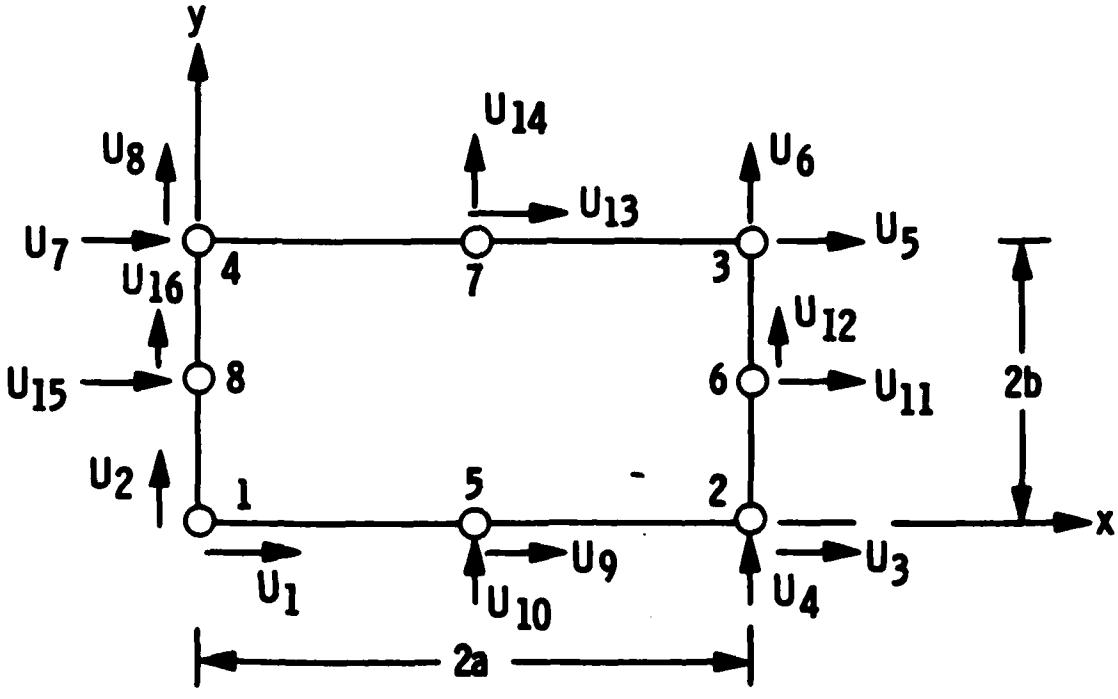

Figure 1. A 8-node plane rectangular element

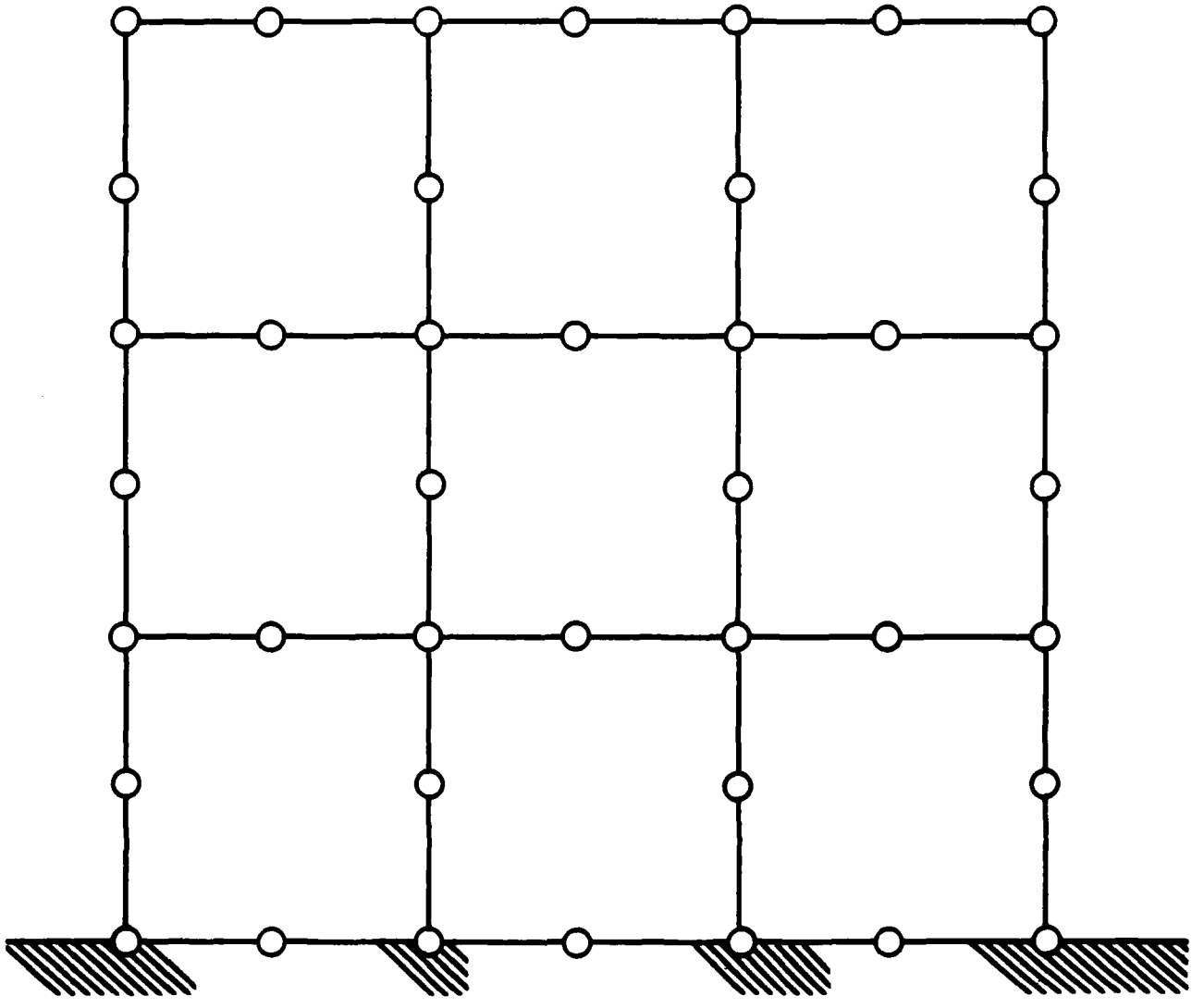

Figure 2. A square plate with plane 8-node elements

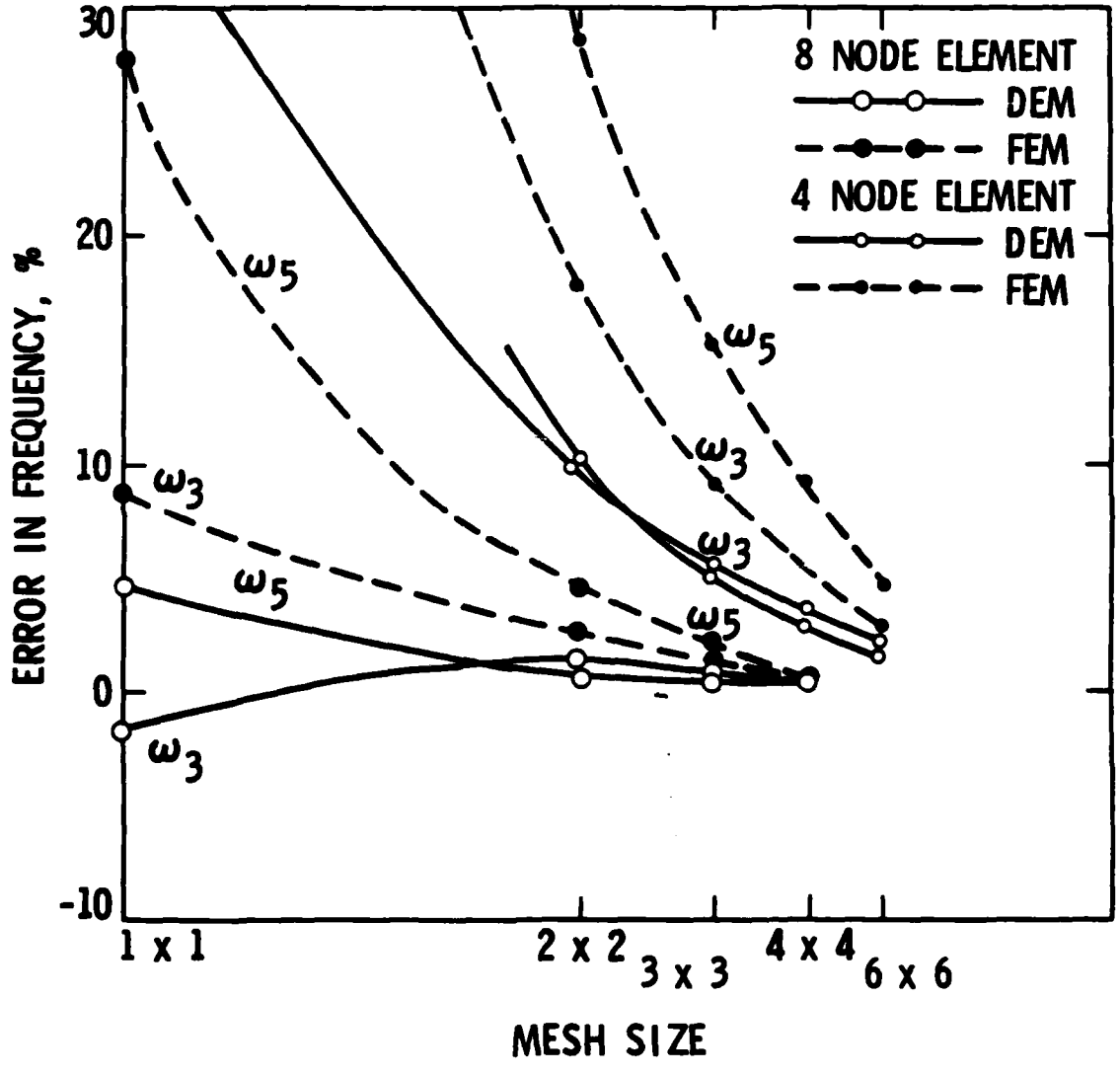

Figure 3. Root convergence comparisons: 8-node and 4-node plane rectangular dynamic and finite elements

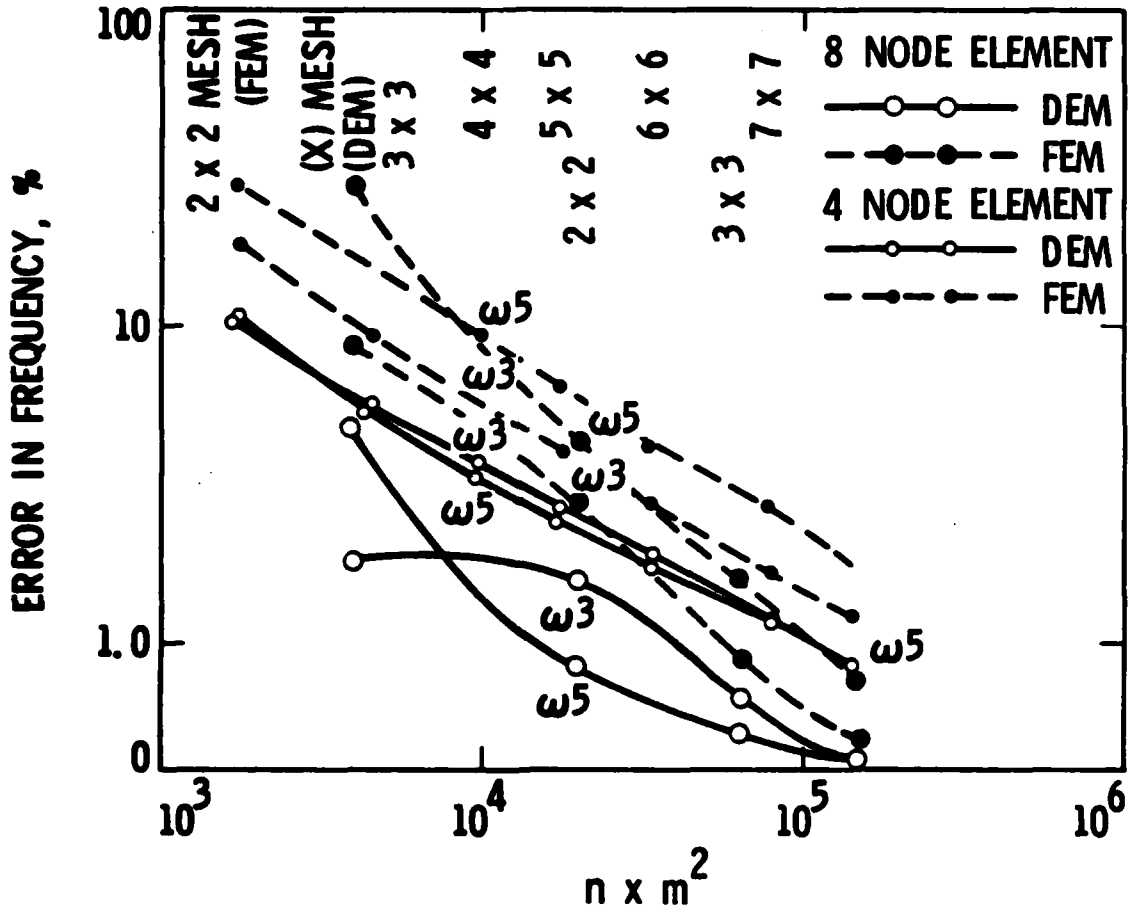

Figure 4. Plane rectangular elements: Comparison of total numerical efforts as a function of error in frequencies

REPORT ON TASK II

"Development of a Solid Hexahedron

Finite Dynamic Element"

(to be published as a full paper)

DEVELOPMENT OF A SOLID HEXAHEDRON FINITE DYNAMIC ELEMENT

A solid hexahedron element, with three translational degrees of freedom per node, is shown in Figure 1. The differential equations of free vibrations of the associated continuum may be expressed as

$$\frac{\partial^2 u_x}{\partial x^2} + \frac{\partial^2 u_x}{\partial y^2} + \frac{\partial^2 u_x}{\partial z^2} + \frac{1}{(1-2\mu)} \frac{\partial}{\partial x}\left(\frac{\partial u_x}{\partial x} + \frac{\partial u_y}{\partial y} + \frac{\partial u_z}{\partial z}\right) = 2(1+\mu)\frac{\rho}{E}\frac{\partial^2 u_x}{\partial t^2} \quad (1)$$

$$\frac{\partial^2 u_y}{\partial x^2} + \frac{\partial^2 u_y}{\partial y^2} + \frac{\partial^2 u_y}{\partial z^2} + \frac{1}{(1-2\mu)} \frac{\partial}{\partial y}\left(\frac{\partial u_x}{\partial x} + \frac{\partial u_y}{\partial y} + \frac{\partial u_z}{\partial z}\right) = 2(1+\mu)\frac{\rho}{E}\frac{\partial^2 u_y}{\partial t^2} \quad (2)$$

$$\frac{\partial^2 u_z}{\partial x^2} + \frac{\partial^2 u_z}{\partial y^2} + \frac{\partial^2 u_z}{\partial z^2} + \frac{1}{(1-2\mu)} \frac{\partial}{\partial z}\left(\frac{\partial u_x}{\partial x} + \frac{\partial u_y}{\partial y} + \frac{\partial u_z}{\partial z}\right) = 2(1+\mu)\frac{\rho}{E}\frac{\partial^2 u_z}{\partial t^2} \quad (3)$$

μ,p,E being the parameters as defined, earlier. Solutions of Eqs. (1), (2) and (3) are taken respectively, as

$$u_x = \sum_{r=0}^{\infty} \omega^r a_{rx} q e^{i\omega t} \quad (4a)$$

$$u_y = \sum_{r=0}^{\infty} \omega^r a_{ry} q e^{i\omega t} \quad (4b)$$

$$u_z = \sum_{r=0}^{\infty} \omega^r a_{rz} q e^{i\omega t} \quad (4c)$$

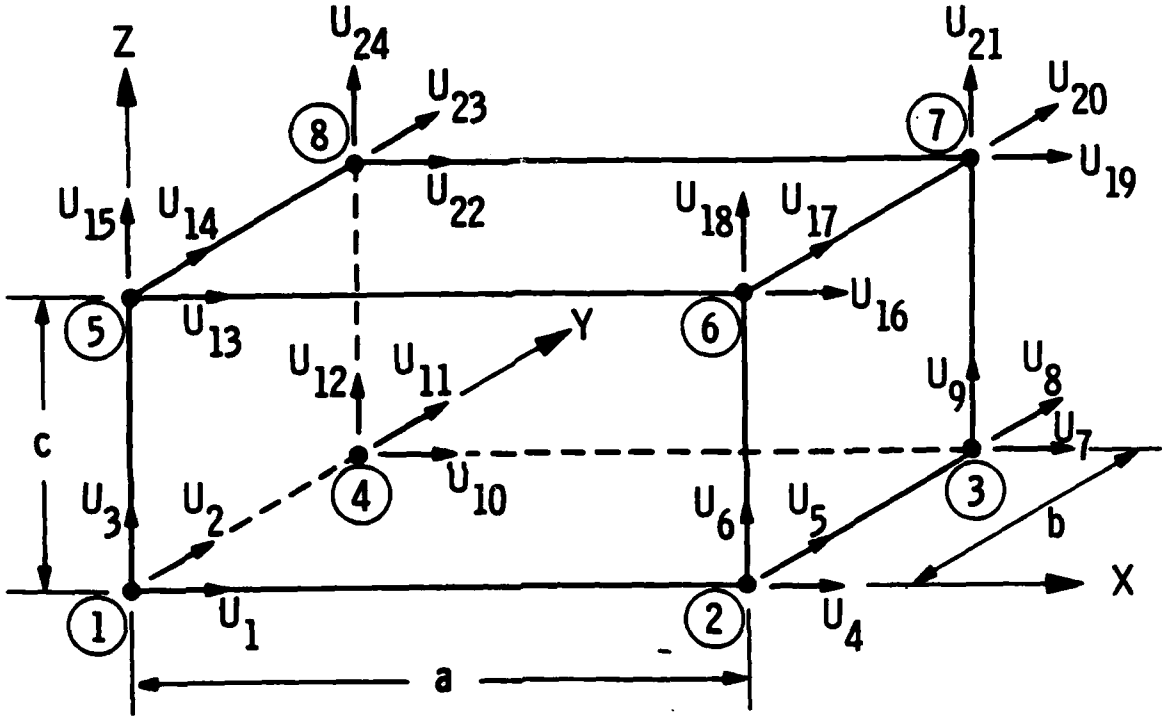

Figure 1 A solid hexahedron element

Retaining only the first three terms in Eqs. 4a, 4b and 4c the shape functions have the following form

$$a_x = a_{0x} + \omega a_{1x} + \omega^2 a_{2x} + \cdots \quad (5)$$

$$a_y = a_{0y} + \omega a_{1y} + \omega^2 a_{2y} + \cdots \quad (6)$$

$$a_z = a_{0z} + \omega a_{1z} + \omega^2 a_{2z} + \cdots \quad (7)$$

which are next substituted into the equilibrium equations to yield the final set of equations of motion by equating the coefficients of the same powers of ω:

x — Direction

$$\frac{\partial^2 a_{0x}}{\partial x^2} + \frac{\partial^2 a_{0x}}{\partial y^2} + \frac{\partial^2 a_{0x}}{\partial z^2} + \alpha_2\left(\frac{\partial^2 a_{0x}}{\partial x^2} + \frac{\partial^2 a_{0y}}{\partial x \partial y} + \frac{\partial^2 a_{0z}}{\partial x \partial z}\right) = 0 \quad (8)$$

$$\frac{\partial^2 a_{1x}}{\partial x^2} + \frac{\partial^2 a_{1x}}{\partial y^2} + \frac{\partial^2 a_{1x}}{\partial z^2} + \alpha_2\left(\frac{\partial^2 a_{1x}}{\partial x^2} + \frac{\partial^2 a_{1y}}{\partial x \partial y} + \frac{\partial^2 a_{1z}}{\partial x \partial z}\right) = 0 \quad (9)$$

$$\alpha_1 \frac{\partial^2 a_{2x}}{\partial x^2} + \frac{\partial^2 a_{2x}}{\partial y^2} + \frac{\partial^2 a_{2x}}{\partial z^2} + \alpha_2\left(\frac{\partial^2 a_{2y}}{\partial x \partial y} + \frac{\partial^2 a_{2z}}{\partial x \partial z}\right) = -\beta a_{0x} \quad (10)$$

y — Direction

$$\frac{\partial^2 a_{0y}}{\partial x^2} + \frac{\partial^2 a_{0y}}{\partial y^2} + \frac{\partial^2 a_{0y}}{\partial z^2} + \alpha_2\left(\frac{\partial^2 a_{0x}}{\partial x \partial y} + \frac{\partial^2 a_{0y}}{\partial y^2} + \frac{\partial^2 a_{0z}}{\partial y \partial z}\right) = 0 \qquad (11)$$

$$\frac{\partial^2 a_{1y}}{\partial x^2} + \frac{\partial^2 a_{1y}}{\partial y^2} + \frac{\partial^2 a_{1y}}{\partial z^2} + \alpha_2\left(\frac{\partial^2 a_{1x}}{\partial x \partial y} + \frac{\partial^2 a_{1y}}{\partial y^2} + \frac{\partial^2 a_{1z}}{\partial y \partial z}\right) \qquad (12)$$

$$\alpha_1 \frac{\partial^2 a_{2y}}{\partial y^2} + \frac{\partial^2 a_{2y}}{\partial x^2} + \frac{\partial^2 a_{2y}}{\partial z^2} + \alpha_2\left(\frac{\partial^2 a_{2x}}{\partial x \partial y} + \frac{\partial^2 a_{2z}}{\partial y \partial z}\right) = -\beta a_{0y} \qquad (13)$$

z — Direction

$$\frac{\partial^2 a_{0z}}{\partial x^2} + \frac{\partial^2 a_{0z}}{\partial y^2} + \frac{\partial^2 a_{0z}}{\partial z^2} + \alpha_2\left(\frac{\partial^2 a_{0x}}{\partial x \partial z} + \frac{\partial^2 a_{0y}}{\partial y \partial z} + \frac{\partial^2 a_{0z}}{\partial z^2}\right) = U \qquad (14)$$

$$\frac{\partial^2 a_{1z}}{\partial x^2} + \frac{\partial^2 a_{1z}}{\partial y^2} + \frac{\partial^2 a_{1z}}{\partial z^2} + \alpha_2\left(\frac{\partial^2 a_{1x}}{\partial x \partial z} + \frac{\partial^2 a_{1y}}{\partial y \partial z} + \frac{\partial^2 a_{1z}}{\partial z^2}\right) = U \qquad (15)$$

$$\alpha_1 \frac{\partial^2 a_{2z}}{\partial z^2} + \frac{\partial^2 a_{2z}}{\partial x^2} + \frac{\partial^2 a_{2z}}{\partial y^2} + \alpha_2\left(\frac{\partial^2 a_{2x}}{\partial x \partial z} + \frac{\partial^2 a_{2y}}{\partial y \partial z}\right) = -\beta a_{0z} \qquad (16)$$

where

$$\alpha_1 = \frac{2(1-\mu)}{(1-2\mu)} \qquad \alpha_2 = 1/(1-2\mu) \qquad \beta = 2(1+\mu)\rho/E$$

Solutions of Equations (8), (11) and (14) are assumed in the following from

$$U_x = a_{0x}U = C_1 + C_2x + C_3y + C_4z + C_5xy + C_6yz + C_7xz + C_8xyz \quad (17)$$

$$U_y = a_{0y}U = C_9 + C_{10}x + C_{11}y + C_{12}z + C_{13}xy + C_{14}yz + C_{15}xz + C_{16}xyz \quad (18)$$

$$U_z = a_{0z}U = C_{17} + C_{18}x + C_{19}y + C_{20}z + C_{21}xy + C_{22}yz + C_{23}xz + C_{24}xyz \quad (19)$$

where the coefficients $C_1 - C_{24}$ are evaluated by appropriate satisfaction of the boundary conditions as below:

$x = 0, y = 0, z = 0$	$u_x = U_{x1} = U_1$	$u_y = U_{y1} = U_2$	$u_z = U_{z1} = U_3$
$x = a, y = 0, z = 0$	$u_x = U_{x2} = U_4$	$u_y = U_{y2} = U_5$	$u_z = U_{z2} = U_6$
$x = a, y = b, z = 0$	$u_x = U_{x3} = U_7$	$u_y = U_{y3} = U_8$	$u_z = U_{z3} = U_9$
$x = 0, y = b, z = 0$	$u_x = U_{x4} = U_{10}$	$u_y = U_{y4} = U_{11}$	$u_z = U_{z4} = U_{12}$
$x = 0, y = 0, z = C$	$u_x = U_{x5} = U_{13}$	$u_y = U_{y5} = U_{14}$	$u_z = U_{z5} = U_{15}$
$x = a, y = 0, z = C$	$u_x = U_{x6} = U_{16}$	$u_y = U_{y6} = U_{17}$	$u_z = U_{z6} = U_{18}$
$x = a, y = b, z = C$	$u_x = U_{x7} = U_{19}$	$u_y = U_{y7} = U_{20}$	$u_z = U_{z7} = U_{21}$
$x = 0, y = b, z = C$	$u_x = U_{x8} = U_{22}$	$u_y = U_{y8} = U_{23}$	$u_z = U_{z8} = U_{24}$

Whereas solutions for equations (9), (12) and (15) are taken in the same form as above, the solutions for equations (10), (13) and (16) are taken as follows:

$$a_2x = A_1 + A_2x + A_3y + A_4z + A_5xy + A_6yz + A_7xz + A_8xyz$$

$$- \left[\frac{C_1x^2}{6\alpha_1} + \frac{C_1y^2}{6} + \frac{C_1z^2}{6} + \frac{C_3x^3}{18\alpha_1} + \frac{C_2xy^2}{6} + \frac{C_2xz^2}{6} + \frac{C_3x^2y}{6\alpha_1} + \frac{C_3y^3}{18} + \frac{C_3yz^2}{6} \right.$$

$$+ \frac{C_4x^2z}{6\alpha_1} + \frac{C_4y^2z}{6} + \frac{C_4z^3}{18} + \frac{C_5x^3y}{18\alpha_1} + \frac{C_5xy^3}{18} + \frac{C_5xyz^2}{6} + \frac{C_6x^2yz}{6\alpha_1} + \frac{C_6y^3z}{18}$$

$$\left. + \frac{C_6yz^3}{18} + \frac{C_7x^3z}{18\alpha 1} + \frac{C_7xy^2z}{6} + \frac{C_7xz^3}{18} + \frac{C_8x^3yz}{18\alpha_1} + \frac{C_8xy^3z}{18} + \frac{C_8xyz^3}{18} \right] \cdot \beta \qquad (20)$$

$$a_{2y} = A_9 + A_{10}x + A_{11}y + A_{12}z + A_{13}xy + A_{14}yz + A_{15}xz + A_{16}xyz$$

$$- \left[\frac{C_9y^2}{6\alpha_1} + C_9\frac{x^2}{6} + C_9\frac{z^2}{6} + C_{10}\frac{xy^2}{6\alpha_1} + \frac{C_{10}x^3}{18} + C_{10}\frac{xz^2}{6} + \frac{C_{11}y^3}{18\alpha_1} + \frac{C_{11}x^2y}{6} \right.$$

$$+ C_{11}\frac{yz^2}{6} + \frac{C_{12}y^2z}{6\alpha_1} + \frac{C_{12}x^2z}{6} + \frac{C_{12}z^3}{18} + \frac{C_{13}xy^3}{18\alpha_1} + C_{13}\frac{x^3y}{18} + C_{13}\frac{xyz^2}{6}$$

$$+ \frac{C_{14}y^3z}{18\alpha_1} + C_{14}\frac{x^2yz}{6} + C_{14}\frac{yz^3}{18} + C_{15}\frac{xy^2z}{6\alpha_1} + C_{15}\frac{x^3z}{18} + C_{15}\frac{xz^3}{18} + C_{16}\frac{xy^3z}{18\alpha_1}$$

$$\left. + C_{16}\frac{x^3yz}{18} + C_{16}\frac{xyz^3}{18} \right] \cdot \beta \qquad (21)$$

$$a_{2z} = A_{17} + A_{18}x + A_{19}y + A_{20}z + A_{21}xy + A_{22}yz + A_{23}xz + A_{24}xyz$$

$$- \left[\frac{C_{17}z^2}{6\alpha_1} + \frac{C_{17}x^2}{6} + C_{17}\frac{y^2}{6} + C_{18}\frac{xz^2}{6\alpha_1} + C_{18}\frac{x^3}{18} + \frac{C_{18}xy^2}{6} + C_{19}\frac{yz^2}{6\alpha_1} + C_{19}\frac{x^2y}{6} \right.$$

$$+ C_{19}\frac{y^3}{18} + C_{20}\frac{z^3}{18\alpha 1} + C_{20}\frac{x^2z}{6} + C_{20}\frac{y^2z}{6} + C_{21}\frac{xyz^2}{6\alpha 1} + C_{21}\frac{x^3y}{18} + C_{21}\frac{xy^3}{18}$$

$$+ C_{22}\frac{yz^3}{18\alpha_1} + C_{22}\frac{x^2yz}{6} + C_{22}\frac{y^3z}{18} + C_{23}\frac{xz^3}{18\alpha_1} + C_{23}\frac{x^3z}{18} + C_{23}\frac{xy^2z}{6}$$

$$\left. + C_{24}\frac{xyz^3}{18\alpha_1} + C_{24}\frac{x^3yz}{18} + C_{24}\frac{xy^3z}{18} \right] \cdot \beta \qquad (22)$$

The strain displacement relationships are given by

$$e = bU$$

in which

$$e = \left\{ e_{xx}\ e_{yy}\ e_{zz}\ e_{xy}\ e_{yz}\ e_{zx} \right\} \qquad (23)$$

the individual strain components being defined as

$$\left.\begin{aligned} e_{xx} &= \frac{\partial U_x}{\partial x} \qquad e_{yy} = \frac{\partial U_y}{\partial y} \qquad e_{zz} = \frac{\partial U_z}{\partial z} \\ e_{xy} &= \frac{\partial U_x}{\partial y} + \frac{\partial U_y}{\partial x} \qquad e_{yz} = \frac{\partial U_y}{\partial z} + \frac{\partial U_z}{\partial y} \qquad e_{xz} = \frac{\partial U_z}{\partial x} + \frac{\partial U_x}{\partial z} \end{aligned}\right\} \qquad (24)$$

Once the shape function matrices and the strain-displacement relations have been derived the mass and stiffness matrices may be formulated in a manner, similar to the preceding section. As before, the MACSYMA program has been extensively used for all algebraic manipulations involved in the development of the various a, b, m and k matrices.

NUMERICAL EXAMPLE

A cube of unit dimensions is chosen as a numerical example. Both finite and dynamic element discretizations were achieved by varying mesh sizes. Results of such analyses are given in Table I.

Table I. Natural frequencies of a cube (FEM and DEM results are shown in upper and lower rows respectively)

Mesh Size	Eigenvalue Parameters					
1x1	.7928	.7930	1.0742	1.7845	2.9197	2.9417
	.7361	.7361	.9883	1.3993	2.1052	2.1052
2x2	.7378	.7381	.9994	1.6947	2.1001	2.1003
	.7228	.7228	.9666	1.5492	1.8761	1.8762
3x3	.7077	.7078	.9598	1.6478	1.9388	1.9389
	.7015	.7015	.9411	1.5777	1.8348	1.8348

The above results indicate that the dynamic elements are significantly more efficient than the corresponding finite elements.

REPORT ON TASK III

a. "Development of a Unified Numerical Procedure for Free Vibration Analysis of Structures", IJNME, 1981.

b. "STARS -- STructural Analysis RoutineS", Data Input Procedure.

STARS (STructural Analysis RoutineS)

K.K.Gupta

DATA INPUT PROCEDURE

PROGRAM DESCRIPTION

Stars is a compact, general-purpose, finite and dynamic element computer program for static (multiple load), free vibration and dynamic response analysis of undamped and damped (viscous and structural) structures including spinning ones.

The element library presently consists of line and triangular/quadrilateral shell elements enabling solution of truss, beam, space frame, plane, plate, shell structures, or any combination thereof. The program allows zero, finite and interdependent deflection boundary conditions. The dynamic response analysis capability allows initial deformation and velocity inputs whereas the transient excitation may be either force of acceleration in nature.

Data input can be at random within a specific data set, and the program offers certain automatic data generation capabilities. Input data is formated as an optimal combination of free and fixed formats.

The program, developed in modular form for easy modifications, is written in FORTRAN for the VAX 11/780 computer and consists of about 6000 instructions. Continued development of the program is envisaged while keeping tight control on the size of the program. Extensive interactive plotting capabilities form an important feature of the program.

DESCRIPTION OF MAINIB INPUT

CARD 1 FORMAT
JOB TITLE
13A6

CARD 2 FORMAT
NN,N,NEL,NMAT,NMECN,NEP,NET,NTMP,NPR,NBUN
FREE FORMAT
WHERE:

NN	= NUMBER OF NODES
N	= ORDER OF PROBLEM (USUALLY 6*NN)
NEL	= TOTAL NUMBER OF ELEMENTS
NMAT	= TOTAL NUMBER OF ELEMENT MATERIAL TYPES
NMECN	= NUMBER OF MATERIAL ELASTIC CONSTANTS
NEP	= TOTAL NUMBER OF ELEMENT PROPERTY TYPES (LINE ELEMENTS)
NET	= TOTAL NUMBER OF ELEMENT THICKNESS TYPES (SHELL ELEMENTS)
NTMP	= TOTAL NUMBER OF ELEMENT TEMPERATURE TYPES
NPR	= TOTAL NUMBER OF ELEMENT PRESSURE TYPES
NBUN	= NUMBER OF NODAL CONNECTIVITY CONDITIONS

CARD 3 FORMAT

IPROB,IBAN,NPREC,NC,IDRS, IPLOT

FREE FORMAT

WHERE:

IPROB = INDEX FOR PROBLEM TYPES, TO BE SET AS FOLLOWS:
- = 1, UNDAMPED FREE VIBRATION CASE FOR NON-SPINNING STRUCTURES.
- = 2, UNDAMPED FREE VIBRATION CASE FOR SPINNING STRUCTURES, C BEING SKEW-SYMMETRIC CORIOLIS MATRIX, K=KE+KG+KC WHERE KE,KG,KC ARE RESPECTIVELY THE ELASTIC, GEOMETRICAL STIFFNESS AND CENTRIFUGAL FORCES MATRIX RESPECTIVELY
- = 3, QUADRATIC MATRIX EIGENPROBLEM OPTION FOR DEM ANALYSIS, K-LAMBDA*M-LAMBDA**2*C, C IS DYNAMIC CORRECTION MATRIX.
- = 4, FOR SPINNING STRUCTURES, WHEN C=CC+CD, CC IS THE SKEW-SYMMETRIC CORIOLIS MATRIX, CD BEING THE DIAGONAL VISCOUS DAMPING MATRIX IN K-I*LAMBDA*C -LAMBDA**2*M FORMULATION.
- = 5, AS IN 4, WITH STRUCTURAL DAMPING, K BEING COMPLEX
- = 6, FOR NON-SPINNING STRUCTURES WITH VISCOUS DAMPING (C).
- = 7, AS IN 6, WITH STRUCTURAL DAMPING
- = 8, SOLVES SIMULTANEOUS EQUATIONS AX=B ONLY, WHEN MATRIX A, REAL SYMMETRIC OR HERMITIAN, IS READ IN LIEU OF K.

IBAN = BANDWIDTH MINIMIZATION OPTION
- = 0, PERFORM MINIMIZATION
- = 1, DO NOT PERFORM MINIMIZATION

NPREC = PRECISION FOR SOLVING PROBLEM
- = 1, SINGLE PRECISION REAL
- = 2, DOUBLE PRECISION REAL
- = 3, SINGLE PRECISION COMPLEX
- = 4, DOUBLE PRECISION COMPLEX

NC = NUMBER OF SETS OF CONCENTRATED NODAL LOAD/MASS DATA (IF NONE SET TO 1)

IDRS = INDEX FOR DYNAMIC RESPONSE ANALYSIS
- = 0, NO RESPONSE ANALYSIS NEEDED
- = 1, PERFORM RESPONSE ANALYSIS

IPLOT = INDEX FOR PLOTTING
- = 0, NO PLOTS ARE REQUIRED
- = 1, PLOT STRUCTURE GEOMETRY; RESTART TO CONTINUE SOLUTION
- = 2, PLOT FINAL NODAL DEFORMATIONS AS FUNCTIONS OF TIME, MODE SHAPES AND ELEMENT STRESSES

```
CARD 4  FORMAT
     IMLUMP,IPLUMP,ISPIN,IPRINT
     FREE FORMAT
     WHERE:
       IMLUMP = INDEX FOR NODAL LUMPED MASS INPUT
              = 0 , NO LUMPED MASS INPUT
              = 1 , LUMPED MASS DATA INPUT (IPROB=1 THRU 7)
       IPLUMP = INDEX FOR NODAL EXTERNAL LOAD INPUT
              = 0 , NO LOAD INPUT
              = 1 , CONCENTRATED NODAL LOAD INPUT (IPROB=8)
       ISPIN  = SPIN OPTION FOR STRUCTURE
              = 0, NO SPIN
              = 1, SPINNING STRUCTURE
       IPRINT = PRINT OUTPUT OPTION
              = 0, FOR FINAL RESULTS OUTPUT ONLY
              = 1, PRINT K,M,C MATRICES AND VALUES OF ROOTS AT VARIOUS
                STAGES OF CONVERGENCE
     NOTE: NODAL MASS MATRIX IS ADDED TO CONSISTENT MASS MATRIX WHICH
           IS A FUNCTION OF DISTRIBUTED MASS DENSITY (RHO) INPUT IN
           EDINPT (VMP MATRIX)


CARD 5  FORMAT  (REQUIRED IF ISPIN=1)
     SV1,SV2,SV3
     FREE FORMAT
     WHERE:
       SV1    = SPIN RATE ALONG GLOBAL X-AXIS (RAD/SEC)
       SV2    = SPIN RATE ALONG GLOBAL Y-AXIS (RAD/SEC)
       SV3    = SPIN RATE ALONG GLOBAL Z-AXIS (RAD/SEC)


CARD 6  FORMAT  (REQUIRED IF IPROB IS NOT EQUAL TO 8)
     INDEX,NR,INORM,PU,PL,ISOLT,INDATA
     FREE FORMAT
     WHERE:
       INDEX  = INDICATOR FOR NUMBER OF EIGENVALUES TO BE COMPUTED.
              = 1, WHEN FIRST NR SMALLEST ROOTS ARE NEEDED.
              = 2, WHEN ALL ROOTS LYING WITHIN LIMITS OF PU AND
                   PL ARE TO BE COMPUTED.
       NR     = NUMBER OF EIGENVALUES TO BE COMPUTED.
       INORM  = THE PARTICULAR DEGREE OF FREEDOM AT WHICH THE VECTOR
                SCALOR IS USED TO NORMALIZE THE EIGENVECTORS.
              = 0, THE ROUTINE NORMALIZES THE VECTORS WITH RESPECT TO
                THE ELEMENT OF Y HAVING LARGEST MODULUS.
              = -1, ELEMENT Y OR YD IS USED FOR NORMALIZATION.
       PU     = UPPER EIGENVALUE LIMIT
       PL     = LOWER EIGENVALUE LIMIT
       ISOLT  = VERSION OF EIGSOL
              = 0 OR 1, STANDARD VERSION
              = 2, SECOND VERSION
       INDATA = INPUT DATA OPTION FOR EIGSOL
              = 0, READ DATA FROM FILE
              = 1, READ DATA FROM CARDS
```

```
CARD 7  FORMAT  (REQUIRED IF IDRS = 1)
     TF,NTTS,IUV,DELT,IDDI
     FREE FORMAT
       TF     = TOTAL TIME SPAN TO EVALUATE DYNAMIC RESPONSE
       NTTS   = TOTAL NUMBER OF SETS OF LOAD/ACCELERATION INPUT DATA
       IUV    = INDEX FOR INITIAL DISPLACEMENT AND VELOCITY INPUT
              = 0, NO INITIAL DISPLACEMENT/VELOCITY INPUT
              = 1, IF EITHER INITIAL DISPLACEMENT OR VELOCITY OR BOTH ARE
                   NON-ZERO
       DELT   = TIME INTERVAL FOR RESPONSE CALCULATION
       IDDI   = INDEX FOR DYNAMIC DATA INPUT
              = 1, NODAL LOAD INPUT
              = 2, NODAL ACCELERATION INPUT


CARD 8  FORMAT  (REQUIRED IF IPROB = 5 OR 7)
     G
     FREE FORMAT
     WHERE:
       G = STRUCTURAL DAMPING PARAMETER (K=K(1+IG))


CARD 9  FORMAT  (REQUIRED IF IPROB = 4 OR 5)
     TO READ DIAGONAL VISCOUS DAMPING MATRIX
     FORMAT (6E10.4)


CARD 10 FORMAT  (REQUIRED IF IPROB = 6 OR 7)
     TO READ ALPHA,BETA
     FORMAT (2E10.4)


CARD 11 FORMAT  (REQUIRED IF IPROB = 6 OR 7 AND ALPHA = BETA = 0.0)
     TO READ BANDED VISCOUS DAMPING MATRIX
     FORMAT (6E10.4)
```

DESCRIPTION OF NODAL DATA (NODCOR) INPUT

(1) INPUT NODAL COORDINATE DATA AT RANDOM
(2) THE FINAL DATA IS AUTOMATICALLY FORMED IN SEQUENCE
(3) IN AUTOMATIC MESH GENERATION, THE IMPOSED DISPLACEMENT BOUNDARY CONDITIONS AND OTHER ELEMENT PROPERTIES OF INTERMEDIATE NODES PERTAIN TO THE LAST CARD OF THE SEQUENCE.
(4) THE THIRD POINT NODES FOR LINE ELEMENTS LYING ON LOCAL X-Y PLANE OF AN ELEMENT MAY BE ANY ACTIVE NODE OR DUMMY ONES PLACED AT THE END OF THE LIST WITH UX=UY=UZ=TX=TY=TZ=0.

CARD FORMAT

NODE	NODAL COORDINATES			NODAL BOUNDARY CONDITIONS						INCR
NO.	X	Y	Z	UX	UY	UZ	TX	TY	TZ	IINC
I5	E10.4	E10.4	E10.4	I5	I5	I5	I5	I5	I5	I5

NOTE:
(1) FOR NODAL BOUNDARY CONDITION
SET VALUE = 0 FOR FREE,
= 1 FOR CONSTRAINED
(2) FOR INCREMENT
SET VALUE = 0 FOR NO INCREMENTATION
= N INCREMENT BY N UNTIL FULL VALUE

PARAMETERS USED IN PROGRAM
(1) IN - NODE NUMBER
(2) VN( ) - NODAL COORDINATES
(3) IIN( ) - NODAL BOUNDARY CONDITIONS
(4) INC( ) - INCREMENT
(5) NN - TOTAL NUMBER OF NODES

EXAMPLE OF INPUT:

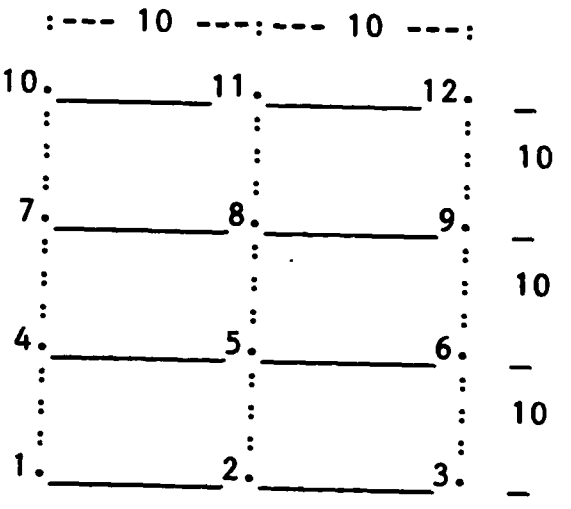

INPUT

1	0.0	0.0	0.0	0	0	1	1	1	1	0
3	20.0	0.0	0.0	0	0	1	1	1	1	1
4	0.0	10.0	0.0	0	0	1	1	1	1	0
10	0.0	30.0	0.0	0	0	1	1	1	1	3
6	20.0	10.0	0.0	0	0	1	1	1	1	0
12	20.0	30.0	0.0	0	0	1	1	1	1	3
5	10.0	10.0	0.0	0	0	1	1	1	1	0
11	10.0	30.0	0.0	0	0	1	1	1	1	3

NOTE: NODES 2,7,9 AND 8 ARE GENERATED

DESCRIPTION OF EDINPT INPUT

(1) INPUT STRUCTURAL ELEMENT DATA AT RANDOM

CARD FORMAT FOR SET (1)

ELEM TYPE	ELEM NO.	NODE 1	NODE 2	NODE 3	NODE 4	NODE 5	NODE 6	NODE 7	NODE 8	IMPP	IEPP /ITHTH	ITMPP	IPRR
LINE 1	*	*	*	**	IEC1	IEC2	FX		+	*	*	*	*
SHELL QUAD 2	*	*	*	*	*				+	*	***	*	*
SHELL TRIA 3	*	*	*	*					+	*	***	*	*

NOTE:

(1) ** FOR THIRD POINT (TYPE 1)
(2) *** FOR ELEMENT THICKNESS TYPE (TYPE 2,3)
(3) + ELEMENT INCREMENT NUMBER FOR AUTOMATIC GENERATION OF INTERMEDIATE ELEMENT DATA BY LINEAR INTERPOLATION, HAVING PROPERTIES SAME AS LAST CARD IN SEQUENCE
(4) FOR LINE ELEMENT - IEC = 1 FOR PIN ENDED, = 0 FOR RIGID ENDED
(5) FX - INITIAL FORCE IN LOCAL X PLANE (TYPE 1)
(6) IMPP - ELEMENT MATERIAL PROPERTY TYPE
(7) IEPP - ELEMENT GEOMETRY PROPERTY TYPE (TYPE 1)
(8) ITMPP - ELEMENT TEMPERATURE PROPERTY TYPE
(9) IPRR - ELEMENT PRESSURE PROPERTY TYPE
(10) ITHTH - ELEMENT THICKNESS PROPERTY TYPE (TYPE 2,3)

FORMAT 14(I5)

CARD FORMAT FOR SET (2), ELEMENT PROPERTY CARD FOR TYPE 1 ONLY

PROP TYPE	A	JX	IY	IZ
I5	E10.4	E10.4	E10.4	E10.4

FORMAT (I5,3E10.4)

NOTE:
(1) A - AREA
(2) JX - TORSIONAL MOMENT OF INERTIA
(3) IY - MOMENT OF INERTIA
(4) IZ - MOMENT OF INERTIA

CARD FORMAT FOR SET (3), ELEMENT THICKNESS DATA CARD FOR TYPE 2,3 ONLY

THICK TYPE	T
I5	E10.4

FORMAT (I5,E10.4)
NOTE:
(1) T - THICKNESS

CARD FORMAT FOR SET (4), ELEMENT MATERIAL PROPERTY CARD
[TO BE SET FOR GENERAL MATERIAL CASE]

MATL TYPE	ELASTIC CONSTANTS						
FOR ISOTROPIC							
*	*(E)	*(MU)	*(ALP)	*(RHO)			
FOR ORTHOTROPIC							
*	*	*	*	*	*	*	*
	*	*	*(ALPX)	*(ALPY)	*(RHO)		
FOR ANISOTROPIC							
*	*	*	*	*	*	*	*
	*	*	*	*	*	*	*
	*	*	*	*	*	*	*
	*(ALPX)	*(ALPY)	*(ALPXY)	*(RHO)			

FORMAT (I5,7E10.4/5X,7E10.4/5X,7E10.4/5X,4E10.4)

NOTE: DATA INPUT IS REQUIRED FOR EACH MATERIAL CASE

CARD FORMAT FOR SET (5), ELEMENT TEMPERATURE INCREMENT CARD

TEMP TYPE	T	DTDY	DTDZ	TEMP TYPE	T	DTDY	DTDZ
I5	E10.4	E10.4	E10.4	I5	E10.4	E10.4	E10.4

FORMAT 2(I5,3E10.4)

NOTE:
(1) T - TEMPERATURE INCREMENT
(2) DTDY - Y-TEMPERATURE GRADIENT
(3) DTDZ - Z-TEMPERATURE GRADIENT

CARD FORMAT FOR SET (6), ELEMENT PRESSURE LOAD CARD

PRESS TYPE	PRESS	PRESS TYPE	PRESS	PRESS TYPE	PRESS	PRESS TYPE	PRESS	PRESS TYPE	PRESS
I5	E10.4	I5	E10.4	I5	E10.4	I5	E10.4	I5	E10.4

FORMAT 5(I5,E10.4)

NOTE:
ELEMENT TYPE 1 - UNIFORM PRESSURE ALLOWED IN LOCAL Y-DIRECTION ONLY
ELEMENT TYPE 2,3 - UNIFORM PRESSURE ALLOWED IN LOCAL Z-DIRECTION ONLY

DESCRIPTION OF GCINPT INPUT

```
SET (1)  INPUT NODAL FORCE (P) OR MASS (M) MATRIX AT RANDOM
         (ONLY IF IPLUMP/IMLUMP NOT EQUAL TO 0)
SET (2)  INPUT DYNAMIC LOADING (ONLY IF IDRS = 1)
SET (3)  INPUT NODAL CONNECTIVITY AT RANDOM


CARD FORMAT FOR SET (1)

     NODE NUMBER    DOF     P OR M
          I5         I5      E10.4
     FORMAT (2I5,E10.4)

     NOTE: (1) FOR NODAL LOAD, EACH CASE IS TERMINATED BY SETTING THE
               NODE NUMBER FOR THE NEXT CASE TO A NEGATIVE NUMBER, SAY -1
           (2) FOR IPROB = 8, IF IPLUMP = 0 THEN TERMINATE INPUT WITH -1


CARD FORMAT FOR SET (2)

CARD 1  FORMAT (REQUIRED IF IUV = 1 AND IDRS = 1)
     TO READ INITIAL DISPLACEMENT/VELOCITY AT RANDOM, TERMINATED BY -1
     FORMAT (2I5,2E15.5)
     NODE NUMBER     DOF     U(I)    V(I)
          *           *       *       *
          .           .       .       .
          .           .       .       .
          .           .       .       .
          *           *       *       *
          -1

CARD 2  FORMAT (REQUIRED IF IDRS = 1 AND NTTS > 0)
     TO READ NTTS NUMBER OF SETS OF NODAL LOAD/ACCELERATION DATA)
     FORMAT (E15.5)
     TZ
     *
     FORMAT (2I5,E15.5)
     NODE NUMBER     DOF    LOAD/ACCELERATION
          *           *           *
          .           .           .
          .           .           .
          .           .           .
          *           *           *
          -1
     NOTE: REPEAT CARD 2 DATA AS AVOVE FOR NTTS NUMBER OF SETS
           EACH TERMINATED BY -1


CARD FORMAT FOR SET (3)

     4(I4,I1,I4,I1,E10.4)
     (NODE  DOF  NODE  DOF  CONNECTIVITY)     4 SETS PER ROW
                            COEFFICIENT
```

FURTHER MAINI INPUT

INPUT OF VISCOUS DAMPING MATRICES

CARD 1 FORMAT (REQUIRED IF IPROB=4 OR 5)
TO READ DIAGONAL VISCOUS DAMPING MATRIX,C(N,1) IN GCS
FORMAT: (6E10.4)

CARD 2 FORMAT (REQUIRED IF IPROB=6 OR 7)
TO READ 'ALPHA' AND 'BETA'
SO THAT [C] = ALPHA*[K] + BETA*[M]
FORMAT: (2E10.4)

CARD 3 FORMAT (REQUIRED IF IPROB=6 OR 7 AND ALPHA=BETA=0.0)
TO READ BANDED VISCOUS DAMPING MATRIX,C(N,M11) IN GCS
FORMAT: (6E10.4)

NOTE: DATA IN CARDS 1 AND 3 MUST CONFORM TO 'ZDBC,FDBC AND IDBC'
INHERENT IN PROBLEM UNDER CONSIDERATION.
WHERE:
ZDBC = ZERO DEFLECTION BOUNDARY CONDITIONS, INPUT IN NODCOR
FDBE = FINITE DEFLECTION BOUNDARY CONDITIONS,
INPUT IN SET (3) IN GCINPT
IDBE = INTERDEPENDENT DEFLECTION BOUNDARY CONDITIONS,
INPUT IN SET (3) IN GCINPT

PARAMETERS USED IN THE PROGRAM

(1) NEL = TOTAL NUMBER OF ELEMENTS
(2) NEP = TOTAL NUMBER OF ELEMENT PROPERTY TYPES (LINE ELEMENTS)
(3) NET = TOTAL NUMBER OF ELEMENT THICKNESS TYPES (SHELL ELEMENTS)
(4) NMAT = TOTAL NUMBER OF ELEMENT MATERIAL TYPES
(5) NMECN = NUMBER OF MATERIAL ELASTIC CONSTANTS
= 4,12,25 FOR ELASTIC ISOTROPIC, ORTHOTROPIC, OR ANISOTROPIC CASE, RESPECTIVELY
(6) NTMP = TOTAL NUMBER OF ELEMENT TEMPERATURE TYPES
(7) NPR = TOTAL NUMBER OF ELEMENT PRESSURE TYPES
(8) IEP( ) = ELEMENT PROPERTY TYPE NUMBER, LINE ELEMENTS (TYPE 1)
(9) VEP(,) = ELEMENT PROPERTIES
(10) IET( ) = ELEMENT THICKNESS TYPE NUMBER, SHELL ELEMENTS (TYPE 2,3)
(11) VET( ) = ELEMENT THICKNESS
(12) IMP( ) = ELEMENT MATERIAL TYPE NUMBER
(13) VMP(,) = ELEMENT ELASTIC CONSTANTS
(14) ITMP( ) = ELEMENT TEMPERATURE TYPE NUMBER
(15) VTMP(,) = ELEMENT TEMPERATURE DATA
(16) IPR( ) = ELEMENT PRESSURE TYPE NUMBER
(17) VPR( ) = ELEMENT PRESSURE DATA

INTERNATIONAL JOURNAL FOR NUMERICAL METHODS IN ENGINEERING, VOL. 17, 187–198 (1981)

DEVELOPMENT OF A UNIFIED NUMERICAL PROCEDURE FOR FREE VIBRATION ANALYSIS OF STRUCTURES†

K. K. GUPTA‡

Jet Propulsion Laboratory, California Institute of Technology, Pasadena, California, U.S.A.

SUMMARY

This paper presents the details of a unified numerical algorithm and the associated computer program developed for the efficient determination of natural frequencies and modes of free vibration of structures. Both spinning and nonspinning structures with or without viscous and/or structural damping may be solved by the current procedure; in addition, the program is capable of solving static problems with multiple load cases as well as the quadratic matrix eigenproblem associated with a finite dynamic element structural discretization. A special symmetric matrix decomposition scheme has been adopted for matrix triangularization, which renders the program rather efficient and economical. Also, a novel bisection scheme is described that further accelerates the solution convergence rate, particularly for the case of repeated roots.

The associated computer program adopts an out-of-core solution strategy, thereby enabling effective solutions to be achieved for large, complex, practical structures. A complete listing of the program written in FORTRAN V, for the UNIVAC 1100/82 computer, along with the source deck is available for ready use.

INTRODUCTION

The dynamic response analysis is of primary importance in the design of a wide range of practical structures, such as spacecraft, buildings, and rotating machineries, among others. A vital preliminary for such an analysis involves the determination of the natural frequencies and the associated modes. This is achieved, first, by discretizing the continuum by a standard technique, such as the finite element method, yielding simultaneous algebraic equations; the resulting eigenvalue problem is then suitably solved to yield the desired roots and vectors. For most complex practical structures, such an idealization results in a rather large number of simultaneous equations, which are usually of highly banded configurations. In order to effect an economical solution, the associated eigenproblem analysis routine must be designed to fully exploit the inherent matrix sparsity. Furthermore, due to the limited core storage available in present computers, it is advantageous to adopt an out-of-core solution strategy that provides effective solutions for practical structures of almost any magnitude and complexity.

While many structures are nonrotating in nature, some are subjected to uniform rotations. Also, such structures may exhibit viscous or structural damping or a combination of both. The associated eigenvalue problems are characterized by distinctive matrix equations. Furthermore, when finite dynamic elements are used for structural discretization, a quadratic matrix

† The research described in this paper was carried out by the Jet Propulsion Laboratory, California Institute of Technology, and was sponsored jointly by the Air Force Office of Scientific Research (AFOSR) and the Large Space Structures Technology (LSST) Project Office at the NASA Langley Research Center.

‡ Member of the Technical Staff, Applied Mechanics Technology Section.

0029–5981/81/020187–12$01.00

Received 28 September 1979
Revised 26 March 1980

eigenvalue formulation is involved. A general formulation unifying the various eigenvalue problems may be presented as

$$\mathbf{M}\ddot{\mathbf{q}} + \mathbf{C}\dot{\mathbf{q}} + \mathbf{K}\mathbf{q} = \mathbf{0} \tag{1}$$

in which $\mathbf{M}$, $\mathbf{C}$ and $\mathbf{K}$ are, in general, the inertia, damping and stiffness matrices, respectively. The individual eigenproblems are identified next.

Case I. Undamped free vibration and buckling

The related matrix formulation becomes

$$\mathbf{M}\ddot{\mathbf{q}} + \mathbf{K}\mathbf{q} = \mathbf{0} \tag{2}$$

the solution of which is taken to be $\mathbf{q} = e^{i\lambda t}$; equation (2) then reduces to

$$(\mathbf{K}_E - \lambda^2\mathbf{M})\mathbf{q} = \mathbf{0} \tag{2a}$$

where $\mathbf{K}_E$ is the elastic stiffness matrix, and λ the natural frequencies. The associated buckling problem is characterized by

$$(\mathbf{K}_E - \hat{\lambda}\mathbf{K}_G)\mathbf{q} = \mathbf{0} \tag{2b}$$

in which $\mathbf{K}_G$ is the geometrical stiffness matrix and $\hat{\lambda}$ the compressive buckling load. The formulation for the associated problem of free vibration of prestressed structures is given by

$$[(\mathbf{K}_E - \mathbf{K}_G) - \lambda^2\mathbf{M}]\mathbf{q} = \mathbf{0} \tag{2c}$$

in which the compressive load is assumed to have a positive sign. Equations (2a)–(2c) are characterized by real roots and vectors since $\mathbf{K}_E$, $\mathbf{K}_G$, $\mathbf{M}$ are real, symmetric matrices, $\mathbf{K}_E$ also being positive definite in nature; for structures exhibiting rigid body motion, a non-negative definite form of $\mathbf{K}_E$ is obtained.

Case II. Undamped free vibration of spinning structures

For undamped structures spinning at a uniform rate Ω, equation (1) assumes the form

$$\mathbf{M}\ddot{\mathbf{q}} + \mathbf{C}_c\dot{\mathbf{q}} + \mathbf{K}\mathbf{q} = \mathbf{0} \tag{3}$$

where $\mathbf{C}_c$ = skew-symmetric Coriolis matrix, being a function of Ω; $\mathbf{K} = \mathbf{K}_E + \mathbf{K}_G + \mathbf{K}'$; $\mathbf{K}_G$ and $\mathbf{K}'$ are the geometrical stiffness and centrifugal forces matrices, respectively, both being functions of Ω^2. The solution (3) is assumed as $\mathbf{q} = e^{pt}$, and the resulting eigenvalue problem takes the form[1]

$$(\mathbf{K} + p\mathbf{C}_c + p^2\mathbf{M})\mathbf{q} = \mathbf{0} \tag{3a}$$

in which p is pure imaginary, such roots and associated complex vectors occurring in conjugate pairs. Further, $\mathbf{K}$ and $\mathbf{M}$ are assumed to be symmetric and positive definite for small vibrations.

Case III. Quadratic matrix equations

If structural discretization is achieved by finite dynamic elements (FDEs), the resulting frequency-dependent stiffness and inertia matrices are, first, expressed in terms of ascending powers of the frequencies λ:

$$\left.\begin{aligned}\mathbf{K} &= \mathbf{K}_0 + \lambda^4\mathbf{K}_4 + \cdots \\ \mathbf{M} &= \mathbf{M}_0 + \lambda^2\mathbf{M}_2 + \cdots\end{aligned}\right\} \tag{4}$$

resulting in the quadratic matrix eigenvalue problem

$$[\mathbf{K}_0 - \lambda^2 \mathbf{M}_0 - \lambda^4 (\mathbf{M}_2 - \mathbf{K}_4)]\mathbf{q} = \mathbf{0} \tag{4a}$$

where $\mathbf{K}_0 = \mathbf{K}_E$, $\mathbf{M}_0 = \mathbf{M}$ are the usual elastic stiffness and mass matrices; $\mathbf{M}_2$, $\mathbf{K}_4$ are the higher order dynamic corrections terms, the inclusion of which in the free vibration analysis is known to effect a significant increase in the solution convergence rate.[2] Equation (4a) is of similar form to equation (3a), but possesses real roots and vectors. Equation (4a) may also be written as

$$(\mathbf{K} - \lambda^2 \mathbf{M} - \lambda^4 \hat{\mathbf{C}})\mathbf{q} = \mathbf{0} \tag{4b}$$

which may be further rearranged as

$$\left(\begin{bmatrix} \hat{\mathbf{C}} & \mathbf{0} \\ \mathbf{0} & \mathbf{K} \end{bmatrix} - \lambda^2 \begin{bmatrix} \mathbf{0} & \hat{\mathbf{C}} \\ \hat{\mathbf{C}} & \mathbf{M} \end{bmatrix} \right) \begin{Bmatrix} \dot{\mathbf{q}} \\ \mathbf{q} \end{Bmatrix} = \mathbf{0} \tag{4c}$$

with $\dot{\mathbf{q}} = \lambda^2 \mathbf{q}$ and which is of the form

$$(\mathbf{E} - \lambda^2 \mathbf{F})\mathbf{y} = \mathbf{0} \tag{4d}$$

where $\mathbf{E}$ and $\mathbf{F}$ are symmetric matrices, $\mathbf{E}$ also being positive definite in nature.

Cases IV and V. Damped free vibration of spinning structures

The associated equations of free vibration without or with structural damping are expressed as

$$\mathbf{M}\ddot{\mathbf{q}} + (\mathbf{C}_c + \mathbf{C}_d)\dot{\mathbf{q}} + \mathbf{K}_E \mathbf{q} = \mathbf{0} \tag{5}$$

$$\mathbf{M}\ddot{\mathbf{q}} + (\mathbf{C}_c + \mathbf{C}_d)\dot{\mathbf{q}} + \mathbf{K}_E (1 + i^* g)\mathbf{q} = \mathbf{0} \tag{6}$$

for cases IV and V, respectively, in which $\mathbf{C}_d$ is the viscous damping matrix assumed to be diagonal, i^* is the imaginary number $\sqrt{-1}$, and g is the structural damping parameter. Substituting $\mathbf{q} = \mathbf{e}^{pt}$ in the above equations, the resulting eigenvalue problems have the following form:

$$[\mathbf{K}_E + p(\mathbf{C}_c + \mathbf{C}_d) + p^2 \mathbf{M}]\mathbf{q} = \mathbf{0} \tag{5a}$$

$$[\mathbf{K}_E (1 + i^* g) + p(\mathbf{C}_c + \mathbf{C}_d) + p^2 \mathbf{M}]\mathbf{q} = \mathbf{0} \tag{6a}$$

in which the roots p, as well as the associated vectors, are obtained as complex conjugate pairs.

Cases VI and VII. Damped free vibration of nonspinning structures

Equation (1) assumes the following form for cases VI and VII, respectively:

$$\mathbf{M}\ddot{\mathbf{q}} + \mathbf{C}\dot{\mathbf{q}} + \mathbf{K}_E \mathbf{q} = \mathbf{0} \tag{7}$$

$$\mathbf{M}\ddot{\mathbf{q}} + \mathbf{C}\dot{\mathbf{q}} + \mathbf{K}_E (1 + i^* g)\mathbf{q} = \mathbf{0} \tag{8}$$

and the related eigenproblem formulations are defined as

$$[\mathbf{K}_E + p\mathbf{C} + p^2 \mathbf{M}]\mathbf{q} = \mathbf{0} \tag{7a}$$

$$[\mathbf{K}_E (1 + i^* g) + p\mathbf{C} + p^2 \mathbf{M}]\mathbf{q} = \mathbf{0} \tag{8a}$$

where the roots and vectors have forms similar to those pertaining to cases IV and V; $\mathbf{C}$ is the viscous damping matrix of general banded form.

Case VIII. Simultaneous equations

Solution of simultaneous equations

$$\mathbf{Sq} = \mathbf{b} \tag{9}$$

is effected, where **S** is either real, symmetric or Hermitian in nature, and **b** is a set of arbitrary vectors. An effective solution of equation (9) is essential in the analysis of the various eigenvalue problems.

The purpose of this paper is to present the details of a unified numerical algorithm and an associated computer program developed for the solution of the above eigenvalue problems defined by cases I to VII. Such a program fully exploits the banded nature of the related matrices and enables computation of only a few desired roots lying within a specified bound without having to compute any other. Since the computer program employs an out-of-core solution strategy, it enables effective solutions to be obtained for complex practical problems of rather large magnitudes. Numerical results are also presented in detail, testifying to the relative efficiency of the present procedure. This is followed by a summary of conclusions.

BASIC NUMERICAL SCHEMES

A solution of the general eigenvalue problem defined by equation (1) is obtained by first rearranging the matrices as follows:

$$\left[\begin{array}{c|c} \mathbf{M} & \mathbf{0} \\ \hline \mathbf{0} & \mathbf{K} \end{array}\right] \left\{\begin{array}{c} \dot{\mathbf{q}} \\ \hline \mathbf{q} \end{array}\right\} + \left[\begin{array}{c|c} \mathbf{0} & -\mathbf{M} \\ \hline \mathbf{M} & \mathbf{C} \end{array}\right] \left\{\begin{array}{c} \ddot{\mathbf{q}} \\ \hline \dot{\mathbf{q}} \end{array}\right\} = \mathbf{0} \tag{10}$$

which may also be written as

$$\mathbf{By} + \mathbf{A}\dot{\mathbf{y}} = \mathbf{0} \tag{11}$$

where

$$\mathbf{y} = \left\{\begin{array}{c} \dot{\mathbf{q}} \\ \hline \mathbf{q} \end{array}\right\} \tag{11a}$$

Substituting $\mathbf{y} = \mathbf{e}^{pt}$ as its solution, equation (11) takes the form

$$(\mathbf{B} + p\mathbf{A})\mathbf{y} = \mathbf{0} \tag{12}$$

which may also be written as

$$(\mathbf{B} - \lambda \mathbf{A}^*)\mathbf{y} = \mathbf{0} \tag{13}$$

where $\lambda = i^* p$ and $\mathbf{A}^* = i^* \mathbf{A}$.

Isolation of roots

For the particular case when $\mathbf{A}^*$ is a Hermitian matrix and **B** is real, symmetric and positive or non-negative definite in nature, the Sturm sequence property[3] is valid for the formulation depicted by equation (13), the associated roots being real in nature. Thus, for a given value of λ, the number of changes in the signs of the leading principal minors $f_r(\lambda)$ is equal to the number of

roots of $\mathbf{B}-\lambda\mathbf{A}^*$ having algebraic values less than λ. As a special case, this property is also valid for the formulation involving a pair of real symmetric matrices. Such a property enables the isolation of only a few desired roots lying within a specified upper and lower bound $[\lambda_u, \lambda_l]$, by a repeated bisection technique, without having to compute any other. Thus, at a particular stage of

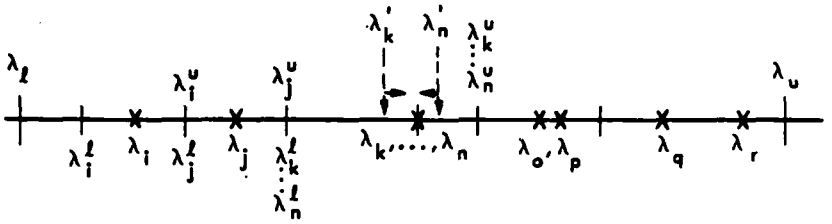

Figure 1. Convergence scheme for repeated roots

computation, the Sturm count determines the number of roots of $\mathbf{B}-\lambda\mathbf{A}^*$, say, x, lying within $[\lambda_m, \lambda_l]$, with $\lambda_m = (\lambda_u + \lambda_l)/2$, λ_u, λ_l being the current upper and lower bounds, respectively. The upper bound of the x roots and the lower bounds of the rest are then set to λ_m, the latter being implemented only if their current lower bounds are smaller than λ_m. The desired roots are automatically isolated and their individual bounds determined when this process is continued. Furthermore, if a number of roots are found within the bound $[\lambda_m, \lambda_l]$, such that the absolute value of $(\lambda_m - \lambda_l)/\lambda_l$ is less than the root separation parameter EPS, then they are considered as repeated ones with a numerical value equal to λ_m. However, the latter process tends to be rather slow for extracting repeated or close roots. A novel strategy has been developed in connection with the present work which essentially reduces the root extraction time for repeated roots to that of distinct ones. Thus, during the bisection process, when monitoring the bounds of a group of roots, if the number of such roots, say, r, remain the same while their upper and lower bounds each changes at least once, then a multiplicity test is immediately carried out. The inverse iteration process described in the next section is then used, employing the respective upper and lower bound values to accurately locate two roots by converging from both ends. If these two root values are found to be identical, the r roots are then asumed to be multiple ones having the numerical value as that of the two converged roots. If, on the other hand, the two converged roots are distinct in values, they are accepted as the true values of the respective roots and the bisection process is continued as usual. This special procedure is depicted in Figure 1, where the roots λ_k to λ_n are repeated in nature. First they are isolated within bounds $[\lambda_k^l, \lambda_n^u]$ when two more bisections are needed to satisfy the criterion for the present strategy. The final bounds λ_k' and λ_n' are then utilized to converge from both sides. This current procedure has been found to be much superior than the usual repeated bisection technique for multiple roots.

For the present set of problems, the Sturm sequence count involving the number of changes in the signs of the leading principal minors is equivalent to counting the number of negative diagonal elements of the decomposed matrix. Depending on the type of problem, such an operation is performed on the following matrix formulation:

Cases I, VI and VII

Matrix triangularization is performed on

$$\mathbf{K}-\lambda^2\mathbf{M} \tag{14}$$

when all operations involve real numbers.

Case III

Similar matrix manipulations are executed with the matrix

$$\mathbf{K}-\lambda^2\mathbf{M}-\lambda^4\hat{\mathbf{C}} \tag{15}$$

also involving real numbers only.

Cases II, IV and V

The decomposition of the matrix

$$\mathbf{K}-i^*\lambda\,\mathbf{C}_c-\lambda^2\mathbf{M} \tag{16}$$

is implemented, when all operations are performed in complex arithmetic.

Location of roots and computation of vectors

Once the roots are isolated by the repeated bisection procedure, an inverse iteration technique is adopted for the simultaneous determination of individual roots and vectors.[3,4] In this process the middle point of the bounds of the isolated rth root is taken as the starting root iteration value:

$$\lambda_m^r=(\lambda_u^r+\lambda_l^r)/2 \tag{17}$$

which is utilized to effect the triangularization of the relevant left-hand side matrix. A starting vector is then chosen to consist entirely of unit real scalars to start matrix iterations; for complex operations, the imaginary parts of the scalars are assumed to be zero. At the end of each iteration a Rayleigh quotient is used to obtain a new estimate of the root under consideration. The matrix formulations adopted for the inverse iteration procedure for a typical iteration are summarized next:

Case I

$$[\mathbf{K}-(\lambda_m^r)^2\mathbf{M}]\mathbf{q}_{i+1}=N_{i+1}\mathbf{M}\mathbf{q}_i^r \tag{18}$$

N_{i+1} being a normalizing factor.

Case II

Lower half of equation (13):

$$[\mathbf{K}-i^*\lambda_m^r\mathbf{C}_c-(\lambda_m^r)^2\mathbf{M}]\mathbf{q}_{i+1}^r=N_{i+1}[\lambda_m^r\mathbf{M}\mathbf{q}_i^r+i^*\mathbf{M}\dot{\mathbf{q}}_i^r+i^*\mathbf{C}_c\mathbf{q}_i^r] \tag{19}$$

Upper half:

$$[\mathbf{M}\dot{\mathbf{q}}_{i+1}^r+i^*\lambda_m^r\mathbf{M}\mathbf{q}_{i+1}^r]=-N_{i+1}\,i^*\mathbf{M}\mathbf{q}_i^r \tag{19a}$$

Case III

Lower half of equation (4d):

$$[\mathbf{K}-(\lambda_m^r)^2\mathbf{M}-(\lambda_m^r)^4\hat{\mathbf{C}}]\mathbf{q}_{i+1}^r=N_{i+1}[\hat{\mathbf{C}}\dot{\mathbf{q}}_i^r+\mathbf{M}\mathbf{q}_i^r+(\lambda_m^r)^2\hat{\mathbf{C}}\mathbf{q}_i^r] \tag{20}$$

Upper half:

$$\hat{\mathbf{C}}\dot{\mathbf{q}}_{i+1}^r-(\lambda_m^r)^2\hat{\mathbf{C}}\mathbf{q}_{i+1}^r=N_{i+1}\hat{\mathbf{C}}\mathbf{q}_i^r \tag{20a}$$

Cases IV and V

Lower half of equation (13):

$$[\mathbf{K}-i^*\lambda_m^r\mathbf{C}_c-(\lambda_m^r)^2\mathbf{M}]\mathbf{q}_{i+1}^r=N_{i+1}[\lambda_m^r\mathbf{M}\mathbf{q}_i^r+i^*\mathbf{M}\dot{\mathbf{q}}_i^r+i^*\mathbf{C}\mathbf{q}_i^r] \tag{21}$$

in which $\mathbf{C}=\mathbf{C}_c+\mathbf{C}_d$.

Upper half: As in case II

Cases VI and VII

Lower half of equation (13):

$$[\mathbf{K}-(\lambda_m^r)^2\mathbf{M}]\mathbf{q}_{i+1}^r=N_{i+1}[\lambda_m^r\mathbf{M}\mathbf{q}_i^r+i^*\mathbf{M}\dot{\mathbf{q}}_i^r+i^*\mathbf{C}\mathbf{q}_i^r] \tag{22}$$

in which $\mathbf{C}$ is the viscous damping matrix of usual banded form.

Upper half: As in case II.

For each root, triangularization of the left-hand side of the above equations is performed only once at the beginning of the iteration. In subsequent iteration steps, their solutions are achieved by the simple back-substitution process.

The Rayleigh quotient is used at each iteration step to achieve a new estimate for the root; their detailed expressions are presented below:

Case I

$$(\lambda_{i+1}^r)^2=(\mathbf{q}_{i+1}^r)^{\mathrm{T}}\mathbf{K}\mathbf{q}_{i+1}^r/(\mathbf{q}_{i+1}^r)^{\mathrm{T}}\mathbf{M}\mathbf{q}_{i+1}^r \tag{23}$$

Case II

$$\lambda_{i+1}^r=(\bar{\mathbf{y}}_{i+1}^r)^{\mathrm{T}}\mathbf{B}\mathbf{y}_{i+1}^r/(\bar{\mathbf{y}}_{i+1}^r)^{\mathrm{T}}\mathbf{A}^*\mathbf{y}_{i+1}^r \tag{24}$$

where

$$(\bar{\mathbf{y}}_{i+1}^r)^{\mathrm{T}}\mathbf{B}\mathbf{y}_{i+1}^r=(\bar{\dot{\mathbf{q}}}_{i+1}^r)^{\mathrm{T}}\mathbf{M}\dot{\mathbf{q}}_{i+1}^r+(\bar{\mathbf{q}}_{i+1}^r)^{\mathrm{T}}\mathbf{K}\mathbf{q}_{i+1}^r \tag{24a}$$

$$(\bar{\mathbf{y}}_{i+1}^r)^{\mathrm{T}}\mathbf{A}^*\mathbf{y}_{i+1}^r=-i^*(\bar{\dot{\mathbf{q}}}_{i+1}^r)^{\mathrm{T}}\mathbf{M}\mathbf{q}_{i+1}^r+i^*(\bar{\mathbf{q}}_{i+1}^r)^{\mathrm{T}}\mathbf{M}\dot{\mathbf{q}}_{i+1}^r+i^*(\bar{\mathbf{q}}_{i+1}^r)^{\mathrm{T}}\mathbf{C}_c\mathbf{q}_{i+1}^r \tag{24b}$$

Case III

$$(\lambda_{i+1}^r)^2=(\mathbf{y}_{i+1}^r)^{\mathrm{T}}\mathbf{E}\mathbf{y}_{i+1}^r/(\mathbf{y}_{i+1}^r)^{\mathrm{T}}\mathbf{F}\mathbf{y}_{i+1}^r \tag{25}$$

where

$$(\mathbf{y}_{i+1}^r)^{\mathrm{T}}\mathbf{E}\mathbf{y}_{i+1}^r=(\dot{\mathbf{q}}_{i+1}^r)^{\mathrm{T}}\hat{\mathbf{C}}\dot{\mathbf{q}}_{i+1}^r+(\mathbf{q}_{i+1}^r)^{\mathrm{T}}\mathbf{K}\mathbf{q}_{i+1}^r \tag{25a}$$

$$(\mathbf{y}_{i+1}^r)^{\mathrm{T}}\mathbf{F}\mathbf{y}_{i+1}^r=(\mathbf{q}_{i+1}^r)^{\mathrm{T}}\hat{\mathbf{C}}\dot{\mathbf{q}}_{i+1}^r+(\dot{\mathbf{q}}_{i+1}^r)^{\mathrm{T}}\hat{\mathbf{C}}\mathbf{q}_{i+1}^r+(\mathbf{q}_{i+1}^r)^{\mathrm{T}}\mathbf{M}\mathbf{q}_{i+1}^r \tag{25b}$$

Case IV

As in case II, but $\mathbf{C}_c$ is replaced by $\mathbf{C}_c+\mathbf{C}_d$.

Case V

As in case IV, but $\mathbf{K}$ is replaced by $\mathbf{K}(1+i^*g)$.

Case VI

As in case II with C replacing $\mathbf{C}_d$.

Case VII

As in case VI, but K is changed to $\mathbf{K}(1+i^*g)$.

The new estimate for λ_{i+1}^r, obtained by using the Rayleigh quotient, is next used to check the pattern of root convergence. Thus, if the factor

$$ACC = \frac{|\lambda_{i+1}^r - \lambda_i^r|}{|\lambda_{i+1}^r|} \tag{26}$$

is found to be smaller than the specified root accuracy parameters EPS1, λ_{i+1}^r is then accepted as the true value of λ^r; otherwise, the above steps involving inverse iterations and calculation of Rayleigh quotients are continued until adequate convergence is achieved.

Repeated real roots are determined entirely by the novel bisection process described earlier. To achieve the associated vectors, these roots are first artificially separated relative to their respective values by an amount $3 \times 2^{-t/2}$, t being the number of digits after the binary point. The inverse iteration procedure is then directly applied to yield the vectors, when, at most, two iterations are required for their accurate determination. Due to extreme sensitivity of eigenvectors to small perturbations in the vicinity of multiple roots, this procedure yields sets of independent vectors corresponding to such roots. The standard Schmidt orthogonalization technique may then be applied to transform the independent vectors into orthogonal ones.

Numerical stability

The triangularization of equations (14)–(22) has been achieved by a symmetric decomposition scheme that omits row interchanges, which, in turn, preserves the bandwidth of the relevant matrices. This reduces the computation time for roots and vectors by a factor between 2 and 3, when compared with similar routines developed earlier.[3,4] Since the matrix equations (14)–(22) are, in general, not positive definite in nature, suitable pivoting was considered to be necessary to preserve numerical stability. In the present work, some alternative measures have been implemented in the program that proves to be effective in preserving numerical stability.

Thus, provided the roots are not required to be calculated to a high precision, the resulting bisection process is remarkably stable in nature and the chances of a breakdown are rather slight.[5] The root accuracy parameters EPS and EPS1 are thus set to 0·0001 and 0·001, respectively, which will result in eigenvalues that are sufficiently accurate for problems usually encountered in practice. Also, the program may easily be run in double precision, if desired, so that a large number of significant figures are retained in subsequent computations. Moreover, if a zero pivot is encountered on any rare occasion, the matrix triangularization may be repeated with a slightly perturbed value of the current λ; however, since the bisection process has proved to be rather well-conditioned, these extra precautions are deemed to be unnecessary.

During the inverse iteration procedure, if a zero pivot is encountered, the program automatically replaces it by ε, the normal rounding error, and continues the process onward. A number of test cases have been run using the program and their convergence characteristics carefully monitored. These results indicate that the program is accurate and reliable in nature.

DEVELOPMENT OF A COMPUTER PROGRAM

A computer program EIGSOL† (EIGen problem SOLution routine), based on the numerical formulations presented in the earlier section, has been developed to achieve efficient solutions to structural free vibration problems. Both spinning and nonspinning structures, with or without viscous and structural damping, as well as the quadratic matrix eigenproblem associated with a finite dynamic element discretization, may be analysed by the program. For spinning structures the program is limited to diagonal viscous damping matrices. An adequate number of comment cards, included in the listing, renders the program to be self-explanatory in nature.

An important aspect of the analysis is related to the solution of simultaneous equations, either real, symmetric or Hermitian, , using an out-of-core solution strategy, and this is effected by the subroutine BANMAT (BANded MATrix solution). The relevant data are all stored in secondary storage units, such as discs, which are brought in the core in suitable predetermined block format. A minimum core storage requirement of (M11, M11) and M11 pertaining to D and AD matrices is required to operate the program BANMAT; M11 is the half bandwidth of K, including the diagonal. The program is designed to run on the 260K UNIVAC 1100/82 computer, which allows usage of up to about 175K core storage, that enables achieving solutions to practical problems of rather large magnitude.

The main driver routine EIGSOL repeatedly calls subroutine INPUT to effect data input. Thus, the upper symmetric halves of K(N, M11), M(N, MB), C (or C_c) (N, MC) and C(N, MCD) are read in predetermined block format; N is the order of the matrices, MB, MC, MCD being the half-bandwidth of M, C, C_d, respectively. Figure 2 shows the arrangement of data blocks, the

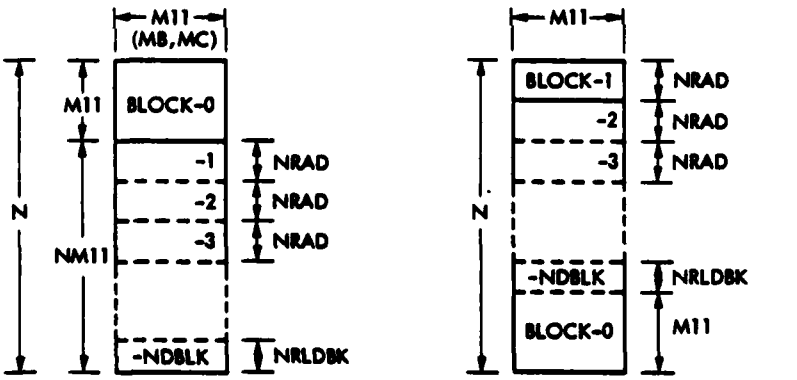

Figure 2. Data block set-up for K, M and C matrices

number of such data blocks (NDBLK) being dependent on the available core area specified by the parameter NAC, which is to be provided by the user. Besides the main store D of dimensions (M11, M11), each block will have NRAD number of rows, the number of such rows in the last data block being defined by NRLDBK. Once the solution has been achieved, it is then stored in the block format, as shown in Figure 2(b).

† The physical program EIGSOL is available from the Computer Management and Information Center (COSMIC), the NASA agency for distribution of computer programs.

Isolation of the desired roots is achieved by the repeated bisection technique effected by the subroutine BISECN, which, in turn, repeatedly calls the subroutine EIGNV to determine the number of roots of the present problem having algebraic values less than the current root value under consideration. The subroutine BANMAT is used by EIGNV for the Sturm sequence count of roots. Once the roots are isolated, they are accurately located by the subroutine VECTOR employing the inverse iteration procedure, which also simultaneously yields the associated vectors. Two other subroutines, MULT and VMULT, are also used by the program for appropriate matrix and vector multiplications.

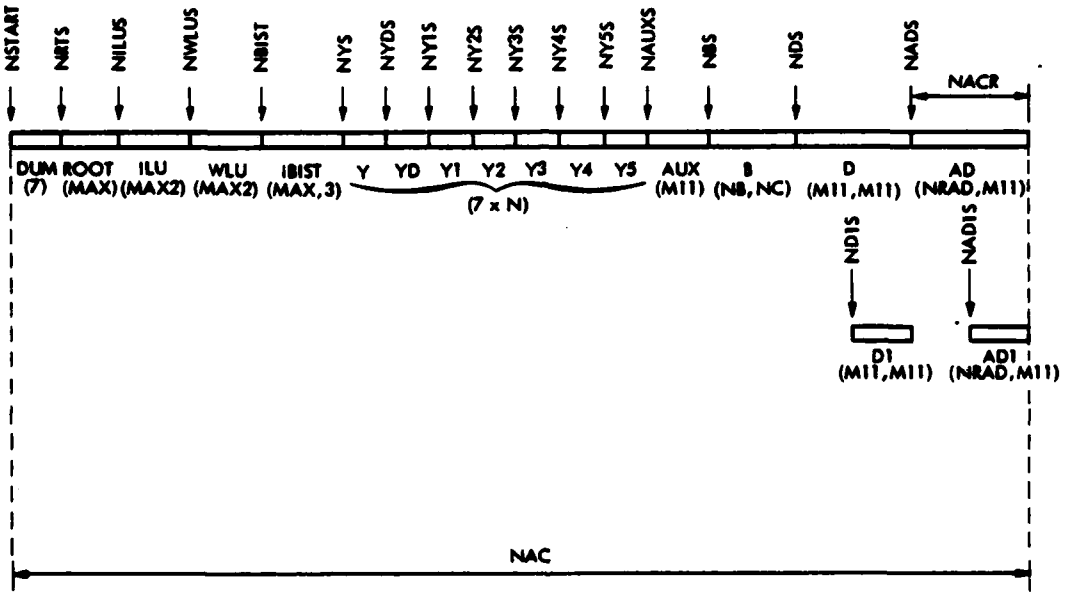

Figure 3. Arrangment of data in common block array A (variables defined in program listing)

Figure 3 depicts the schematic arrangement of data in the main common block core, containing an array A that contains all major vectors and matrices. The starting addresses of theses arrays relative to the array A are also shown in the figure, which are used in the arguments of the various subroutines called by the main driver routine to effect appropriate equivalence of these arrays with array A. This common block is designed in such a way that it occupies the last portion of the computer data bank (DBANK). Thus, as long as A has at least a starting address in the first core module of the computer, it will automatically spill over to the other data banks, enabling utilization of about 175K core memory in a 260K UNIVAC 1100/82 machine. Thus, the program is capable of solving rather large practical problems. Depending on the nature of the problem, the program operates either in real or complex mode.

NUMERICAL RESULTS

An extensive number of test cases have been solved by the program EIGSOL to check out the various capabilities offered by the procedure as well as to establish the relative efficacy of the

program in comparison to other existing ones. Thus, the spinning cantilever beam problem, presented earlier,[3] is again chosen as a numerical example. The basic elastic properties of the beam, divided in 10 discrete elements of length l and expressed in the inch-pound-second unit system, are as follows:

Moment of inertia (Y-axis)	$=\frac{1}{12}$
Moment of inertia (Z-axis)	$=\frac{1}{24}$
Area of cross-section	$=1{\cdot}0$
Young's modulus	$=30\times10^6$
Nodal mass in translation	$=1$
Nodal mass moment of inertia	$=\frac{1}{33}$
Scalar viscous damping	$=0{\cdot}628318$
Structure damping parameter (g)	$=0{\cdot}01$
Element length (l)	$=6$

where the direction of the X-axis is chosen along the length of the beam. A number of computer runs were performed corresponding to problem cases II, IV and V by setting the appropriate input parameter IPROB to 2, 4 and 5, respectively. The beam was subjected to a uniform spin rate $\Omega = 0{\cdot}1$ Hz, along the Y-axis, at the built-in end; the results of such analyses are summarized in Table I. Each analysis, involving the first six roots and associated vectors, required about 16 sec of CPU time using the UNIVAC 1100/82 computer, in which all relevant matrices pertaining to the various formulations have been taken into consideration.

Table I. Spinning cantilever beam: natural frequencies for various problem types for a spin rate $\Omega = 0{\cdot}1$ Hz

Mode	Structure without damping (IPROB = 2)	Structure with viscous damping (IPROB = 4)	Structure with viscous and structural damping (PROB = 5)
1	2·3955	$-0{\cdot}3092 \pm 2{\cdot}3548i^*$	$-0{\cdot}3199 \pm 2{\cdot}3506i^*$
2	3·5689	$-0{\cdot}3121 \pm 3{\cdot}5414i^*$	$-0{\cdot}3287 \pm 3{\cdot}5364i^*$
3	15·2142	$-0{\cdot}3167 \pm 15{\cdot}2077i^*$	$-0{\cdot}3912 \pm 15{\cdot}1964i^*$
4	21·7754	$-0{\cdot}3166 \pm 21{\cdot}7708i^*$	$-0{\cdot}4252 \pm 21{\cdot}7643i^*$
5	43·0167	$-0{\cdot}32021 \pm 43{\cdot}0143i^*$	$-0{\cdot}5340 \pm 43{\cdot}0298i^*$
6	61·0008	$-0{\cdot}32022 \pm 60{\cdot}9992i^*$	$-0{\cdot}6249 \pm 60{\cdot}9880i^*$

To check out the program for cases VI and VII, a taut string vibration problem[3] was analysed using the EIGSOL program. The results were in very good agreement with that presented in Reference 3, the relative solution time being reduced by a factor of about 2·3. A suitable problem pertaining to the quadratic matrix equations (case III) was also checked out by the present program. A cantilever plate free vibration problem[4] of aspect ratio 1:2, involving matrices of order 432, was also solved to check out problems defined by case I. The solution time for the first six roots and vectors was found to be about 1 min of CPU time, compared to that of 2·5 min using the program EASI of Reference 4.

CONCLUDING REMARKS

A unified numerical procedure has been presented for the efficient solution of free vibration problems of usual and spinning structures with or without various forms of damping. Such a

formulation also includes the quadratic matrix eigenvalue problem associated with the finite dynamic element discretization.

The program fully exploits matrix sparsity, such as bandedness, and enables computation of only a few desired roots and vectors without having to compute any other. In general, when run on the same computer, the present program is found to be over two times faster than the related programs DAMP,[3] EASI[4] and QMESSI.[2] The program adopts an out-of-core solution strategy, and as such it is capable of solving large, complex, practical problems. Since the eigenproblem solution time is proportional to $N \times M11^2$, it is highly desirable to adopt a suitable bandwidth minimization scheme to achieve a minimum value for M11 before utilizing the EIGSOL routine. It is hoped that the present program will be developed further into a small general-purpose finite element computer procedure in the near future.

ACKNOWLEDGEMENT

The work was sponsored by an Air Force Office of Scientific Research Grant No. AFOSR 77-3276, under the management of Lt. Col. Carl Edward Oliver, whose support and encouragement are gratefully acknowledged.

REFERENCES

1. J. S. Przemieniecki, *Theory of Matrix Structural Analysis*, McGraw-Hill, New York, 1968.
2. K. K. Gupta, 'Development of a finite dynamic element for free vibration analysis of two-dimensional structures', *Int. J. num. Meth. Engng*, 12, 1311–1327 (1978).
3. K. K. Gupta, 'Eigenproblem solution of damped structural systems', *Int. J. num. Meth. Engng*, 8, 877–911 (1974).
4. K. K. Gupta, 'Eigenproblem solution by a combined Sturm sequence and inverse iteration technique', *Int. J. num. Meth. Engng*, 7, 17–42 (1973).
5. J. H. Wilkinson, *The Algebraic Eigenvalue Problem*, Clarendon Press, Oxford, 1965.

REPORT ON ADDITIONAL EFFORT

"Free Vibration Analysis of Coupled Fluid-Structure Systems", Invited paper, Proceedings of the "Fourth International Symposium on Finite Element Methods in Flow Problems", Tokyo, July 1982.

FINITE ELEMENT FLOW ANALYSIS

Proceedings of the Fourth International Symposium on
Finite Element Methods in Flow Problems
held at Chuo University, Tokyo, on July 26-29, 1982

edited by
TADAHIKO KAWAI

UNIVERSITY OF TOKYO PRESS

FREE VIBRATION ANALYSIS OF COUPLED FLUID-STRUCTURE SYSTEMS

K. K. GUPTA

Jet Propulsion Laboratory,
California Institute of Technology,
Pasadena, California 91109, U.S.A.

SUMMARY

This paper is concerned with the free vibration analysis of coupled fluid-structure systems, discretized by the finite element method. Both compressible and incompressible fluids are considered in the analysis, the latter being a special case of the first one. A numerical analysis procedure, based on an inverse iteration technique in conjuction with a special bisection scheme exploiting the Sturm sequence property, is described in this paper that enables computation of the desired roots and vectors of the vibrating coupled system without having to compute any other. Further, the procedure utilizes the associated structural stiffness and mass matrices as well as the fluids counterpart matrices in their orginal banded form, thereby effecting efficient solution of the eigenvalue problem.

INTRODUCTION

A large number of practical structures are required to withstand externally applied dynamic loadings. The vital preliminary for such a design requires the free vibration analysis of the structures, involving, by far, the major amount of computation time of the entire analysis effort. Many structures exhibit coupled fluid-structure interactions, excellent accounts of which are narrated in References 1 and 2. The first category of such a phenomenon is characterized by large fluid motion, an important example being the flutter of aircraft wings. Some numerical solution procedures of such problems have been presented earlier[3,4].

In the second category, the fluid is assumed to undergo only finite displacement, the motion being limited to small amplitudes. By employing a finite element discretization, the free vibration problem of a fluid-structure resonant system may be writen as[5]

$$\underline{K}\,\underline{u} - \omega^2\underline{M}\,\underline{u} - \underline{C}\,\underline{p} = 0 \qquad \ldots(1)$$

$$\underline{H}\,\underline{p} - \omega^2\underline{Q}\,\underline{p} - \omega^2\rho\underline{C}^T\underline{u} = 0 \qquad \ldots(2)$$

where

- $\underline{K}$ = structural stiffness matrix
- $\underline{M}$ = structural inertia matrix
- $\underline{H}$ = fluid matrix associated physically with the inertia properties of the fluid (analogous to $\underline{K}$)
- $\underline{Q}$ = fluid matrix associated with its compressible behavior (analogous to $\underline{M}$)
- $\underline{C}$ = fluid-structure coupling matrix, sparse and rectangular in nature
- $\underline{u}$ = structural nodal deformation vector

$\underline{p}$ = fluid nodal pressure vector
ρ = fluid density

and in which the fluid idealization is accomplished by the standard Eulerian pressure formulation, the fluid being assumed to be inviscid and compressible in nature. The $\underline{Q}$ matrix formulation includes the coefficient denoting the speed of sound in the fluid medium. Equations (1) and (2) may be combined, as below, yielding the finite element fluid-structure eigenvalue problem of the entire system[5]

$$\left(\begin{bmatrix} \underline{K} & -\underline{C} \\ \underline{0} & \underline{H} \end{bmatrix} - \omega^2 \begin{bmatrix} \underline{M} & \underline{0} \\ \rho \underline{C}^T & \underline{0} \end{bmatrix} \right) \begin{Bmatrix} \underline{u} \\ \underline{p} \end{Bmatrix} = \{0\} \qquad \ldots(3)$$

which may be solved by standard procedure involving real matrices. However, because of the unsymmetric nature of the above matrices, the solution tends to be rather inefficient and uneconomical in nature. An earlier effort[6] succeeded in reformulating equation (3) in a symmetric form, although the entire solution process still required a considerable amount of computational effort.

In the particular case when the fluid is assumed as incompressible, a simplification in the eigenproblem formulation may be achieved. Thus, in the absense of the $\underline{Q}$ matrix an expression for $\underline{p}$ is obtained from the reduced equation (3), which on substitution in equation (1) yields the corresponding eigenvalue problem

$$[\, \underline{K} - \omega^2 (\underline{M} + \rho \underline{C}\, \underline{H}^{-1} \underline{C}^T)]\, \underline{u} = \underline{0} \qquad \ldots(4)$$

which has the effect of adding an additional mass matrix to the structural eigenproblem formulation. The final mass matrix, however, tends to possess a rather large bandwidth if the number of degrees of freedom at the interface happens to be large, which in turn proves to be expensive for the corresponding natural frequency analysis. A solution procedure for equation (4), based on the inverse iteration method is presented in Reference 7.

The purpose of this paper is to present an efficient numerical technique for the eigenproblem solution of the compressible fluid-structure interaction problem defined by equation (3). The procedure starts with the natural frequency analysis of the structure in the absence of any fluid. This is achieved by a combined Sturm sequence and inverse iteration technique that computes only the required eigenvalues and vectors. A special inverse iteration scheme is next developed for the coupled system that utilizes the eigenvalues, computed earlier, as starting iteration values for convergence to the required roots and vectors. The solution process takes full advantage of the relationship in the relative frequency values of the structure without any fluid, structure with incompressible and compressible fluids respectively. Numerical results obtained by solving a number of standard test cases clearly indicate the pattern of root convergence corresponding to various simplifying assumptions, further demonstrating the relative efficiency of the present procedure.

DEVELOPMENT OF NUMERICAL PROCEDURE

To achieve an effective solution of the eigenvalue problem under consideration, equation (3) is first rearranged as follows:

$$\left[\begin{array}{c|c} \underline{H} & \underline{0} \\ \hline -\underline{C} & \underline{K} \end{array}\right] \left\{\begin{array}{c} \underline{p} \\ \hline \underline{u} \end{array}\right\} - \omega^2 \left[\begin{array}{c|c} \underline{0} & \rho\underline{C}^T \\ \hline \underline{0} & \underline{M} \end{array}\right] \left\{\begin{array}{c} \underline{p} \\ \hline \underline{u} \end{array}\right\} = \underline{0} \qquad \ldots(4)$$

which may also be written as

$$(\underline{F} - \lambda\underline{E})\underline{Y} = \underline{0} \qquad \ldots(5)$$

where

$$\lambda = \omega^2 \ , \quad \underline{Y} = \left\{\begin{array}{c} \underline{p} \\ \hline \underline{u} \end{array}\right\} . \qquad \ldots(5a)$$

Subsequent analysis procedure is based on an implicit assumption that the roots computed for the structure ($\lambda_i^{(S)}$), structure with incompressible fluid ($\lambda_i^{(I)}$) and structure wit' compressible fluid ($\lambda_i^{(C)}$) bear the following relationship[8,9]

$$\lambda_i^{(S)} > \lambda_i^{(I)} > \lambda_i^{(C)} \qquad \ldots(6)$$

which proves to be useful in the determination of any desired roots and vectors.

The entire solution process consists of the following major steps

Step 1

Solve $(\underline{K} - \lambda\underline{M})\underline{u} = \underline{0}$, the eigenvalue problem pertaining to the structure only to yield $\lambda_i^{(S)}$ and $\underline{Y}_i^{(S)}$, employing a combined Sturm sequence and inverse iteration procedure[10].

Step 2

For each root determined in step 1 solve $(\underline{F} - \lambda_i^{(S)}\underline{E})\underline{Y} = \underline{0}$, the eigenvalue problem for the incompressible fluid-structure combination by setting $\underline{0} = \underline{0}$ to obtain a reduced $\underline{E}$ matrix denoted by $\underline{E}$. The solution is achieved by an inverse iteration scheme and a bisection strategy, described in detail later, by employing $\lambda_i^{(S)}$ and $\underline{Y}_i^{(S)}$ as the starting iteration root and vector respectively, yielding sets of $\lambda_i^{(I)}$ and $\underline{Y}_i^{(I)}$.

Step 3

Solve $(\underline{F} - \lambda_i^{(I)}\underline{E})\underline{Y} = \underline{0}$, pertaining to the compressible fluid-structure case by employing $\lambda_i^{(I)}$ and $\underline{Y}_i^{(I)}$ as the starting iteration parameters, as in step 2, yielding the desired root $\lambda_i^{(C)}$

and vector $\underline{Y}_i^{*(C)}$.

Step 4

Triangularize $(\underline{F} - \lambda_i^{*(C)}\underline{E})$ and perform a Sturm sequence count to determine the sequence of $\lambda_i^{*(C)}$ in the eigenspectrum (say rth). Then perform a bisection procedure based on the strategy as below:

(i) If r=i then $\lambda_i^{(C)} = \lambda_i^{*(C)}$ and repeat steps 2 and 3 for the next desired root.

(ii) If r > i then repeat the inverse iteration procedure with $\lambda = (\lambda_i^{(I)} + \lambda_{i-1}^{(I)})/2$ or $\left(\lambda_i^{(S)} - \lambda_{i-1}^{(S)}\right)/2$ (if step 2 has been omitted from consideration) to converge to the required ith root $\lambda_i^{(C)}$ and the corresponding vector $\underline{Y}_i^{(C)}$.

Step 5

Repeat step 4 if r > i+1 till all roots up to the ith one and the corresponding vectors are recovered. Assume $\lambda_i^{(C)} = \lambda_i^{(C)}$.

Step 6

Repeat steps 2 through 5 till all required roots and vectors are computed.

The inverse iteration scheme, implicit in the above steps, is carried out by utilizing equation (5). Thus the iteration at the rth step is performed on the following matrix formulation

$$(\underline{F} - \lambda_i\underline{E})\underline{Y}_i^{r+1} = N_i^{r+1}\underline{E}\,\underline{Y}_i^{r} \qquad \ldots(7)$$

which may also be written as

$$\left[\begin{array}{c|c} \underline{H}-\lambda_i\underline{Q} & -\lambda_i\rho\underline{C}^T \\ \hline -\underline{C} & \underline{K}-\lambda_i\underline{M} \end{array}\right] \left\{\begin{array}{c} \underline{p}_i^{r+1} \\ \hline \underline{u}_i^{r+1} \end{array}\right\} = N_i^{r+1} \left[\begin{array}{c} \underline{Q}\,\underline{p}_i^{r} + \rho\underline{C}^T\underline{u}_i^{r} \\ \hline \underline{M}\,\underline{u}_i^{r} \end{array}\right] \qquad \ldots(8)$$

where N_{i+1} is a normalizing factor. Solution of equation (8) is achieved by first writing the matrix equation corresponding to the lower and upper half, respectively, as below

$$(\underline{K} - \lambda_i\underline{M})\underline{u}_i^{r+1} - \underline{C}\,\underline{p}_i^{r+1} = N_i^{r+1}\underline{M}\,\underline{u}_i^{r} \qquad \ldots(9)$$

$$(\underline{H} - \lambda_i\underline{Q})\underline{p}_i^{r+1} - \lambda_i^{r}\rho\underline{C}^T\underline{u}_i^{r+1} = (\underline{Q}\,\underline{p}_i^{r} + \rho\underline{C}^T\underline{u}_i^{r})N_i^{r+1} \qquad \ldots(10)$$

The procedure starts by solving equation (9) with the right hand vector $\underline{Y}$ assumed to be consisting entirely of unit scalars. Equation (10) is then solved for the $\underline{p}$ vector and the process being repeated till adequate convergence is assured. The associated root is then simply computed from the Rayleigh quotient:

$$\lambda_i = (\underline{Y}_i^{r+1})^T \underline{F}\, \underline{Y}_i^{r+1} \Big/ (\underline{Y}_i^{r+1})^T \underline{E}\, \underline{Y}_i^{r+1} \qquad \ldots(11)$$

Triangularization of the relevant matrix pertaining to step 2 is obtained by setting $\underline{Q} = \underline{0}$ in equation (8). Indeed, step 2 may be entirely omitted for compressible fluid, thereby effecting further saving in solution time.

NUMERICAL RESULTS

A computer program has been developed for the natural frequency analysis of fluid-structure systems, which is capable of computing the desired roots and vectors of the coupled system in an efficient manner. The example problem of dry dock in Reference 5 was solved by the program as a test case, and the results correlated rather well. Such solution results were printed out at various analysis steps to verify the efficacy of the bisection procedure adopted for the present analysis, and such results confirm the reliable nature of the numerical algorithm.

CONCLUDING REMARKS

A numerical procedure has been presented that proves to be efficient for the free vibration analysis of fluid-structure coupled systems. The fluid is assumed to be compressible in nature and the incompressible problem is only a special case of the generalized algorithm developed in the paper.

From the numerical formulation depicted by equations 7-11 it is apparent that the current procedure employs the individual $\underline{K}$, $\underline{M}$, $\underline{H}$, $\underline{Q}$, and $\underline{C}$ matrices in their original banded form and thus fully exploits the inherent matrix sparsity usually associated with a finite element formulation. The usual procedures, such as proposed in references 6 and 9, involve various matrix inversions that finally requires solution of eigenvalue problems characterized by full matrices. A similar situation is also encountered with the approximate formulation for incompressible fluid. The present procedure also enables computation of a few roots and vectors only without having to compute any other.

ACKNOWLEDGMENT

The work was sponsored by an Air Force Office of Scientific Research Grant No. AFOSR 80-0169, under the management of Lt. Col. Carl Edward Oliver, whose support and encouragement are gratefully acknowledged.

REFERENCES

1 O. C. Zienkiewicz and P. Bettess: "Fluid-Structure Dynamic Interaction and Wave Forces: An Introduction to Numerical Treatment," Int. J. Num. Meth. Engng., vol.13, 1978, pp. 1-16.

2 O. C. Zienkiewicz: "The Finite Element Method in Engineering Science," McGraw-Hill, England, 1971

3 M. D. Olson: "Some Flutter Solution Using Finite Elements," J. AIAA, vol.8, 1970, pp. 747-752.

END

FILMED

3-83

DTIC